



This discussion paper is/has been under review for the journal Geoscientific Model Development (GMD). Please refer to the corresponding final paper in GMD if available.

A simulation model to assess groundwater recharge over Europe's karst regions

A. Hartmann^{1,3}, T. Gleeson², R. Rosolem¹, F. Pianosi¹, Y. Wada⁴, and T. Wagener¹

¹Department of Civil Engineering, University of Bristol, Bristol, UK

²Civil Engineering, McGill University, Montréal, Canada

³Faculty of Environment and Natural Resources, University of Freiburg, Freiburg, Germany

⁴Department of Physical Geography, Utrecht University, Utrecht, the Netherlands

Received: 25 September 2014 – Accepted: 30 October 2014 – Published: 19 November 2014

Correspondence to: A. Hartmann (aj.hartmann@bristol.ac.uk)

Published by Copernicus Publications on behalf of the European Geosciences Union.

GMDD

7, 7887–7935, 2014

Simulation of groundwater recharge over Europe's karst regions

A. Hartmann et al.

[Title Page](#)

[Abstract](#)

[Introduction](#)

[Conclusions](#)

[References](#)

[Tables](#)

[Figures](#)

◀

▶

◀

▶

[Back](#)

[Close](#)

[Full Screen / Esc](#)

[Printer-friendly Version](#)

[Interactive Discussion](#)

Abstract

Karst develops through the dissolution of carbonate rock and is a major source of groundwater contributing up to half of the total drinking water supply in some European countries. Previous approaches to model future water availability in Europe are either too-small scale or do not incorporate karst processes, i.e. preferential flow paths. This study presents the first simulations of groundwater recharge in all karst regions in Europe with a parsimonious karst hydrology model. A novel parameter confinement strategy combines a priori information with recharge-related observations (actual evapotranspiration and soil moisture) at locations across Europe while explicitly identifying uncertainty in the model parameters. Europe's karst regions are divided into 4 typical karst landscapes (humid, mountain, Mediterranean and desert) by cluster analysis and recharge is simulated from 2002 to 2012 for each karst landscape. Mean annual recharge ranges from negligible in deserts to $> 1 \text{ m a}^{-1}$ in humid regions. The majority of recharge rates ranges from 20–50 % of precipitation and are sensitive to sub-annual climate variability. Simulation results are consistent with independent observations of mean annual recharge and significantly better than other global hydrology models that do not consider karst processes (PCR-GLOBWB, WaterGAP). Global hydrology models systematically underestimate karst recharge implying that they over-estimate actual evapotranspiration and surface runoff. Karst water budgets and thus information to support management decisions regarding drinking water supply and flood risk are significantly improved by our model.

1 Introduction

Groundwater is the main source of water supply for billions of people in the world (Gleeson et al., 2012). Carbonate rock regions constitute about 35 % of Europe's land surface (Williams and Ford, 2006), yet up to 50 % of the national water supply in some European countries (COST, 1995) because of their high storage capacity and

Simulation of groundwater recharge over Europe's karst regions

A. Hartmann et al.

[Title Page](#)

[Abstract](#)

[Introduction](#)

[Conclusions](#)

[References](#)

[Tables](#)

[Figures](#)

◀

▶

◀

▶

[Back](#)

[Close](#)

[Full Screen / Esc](#)

[Printer-friendly Version](#)

[Interactive Discussion](#)



permeability (Ford and Williams, 2007). Climate simulations suggest that in the next 90 years Mediterranean regions will be exposed to higher temperatures and lower precipitation amounts (Christensen et al., 2007). In addition, shifts in hydrological regimes (Milly et al., 2005) and hydrological extremes (Dai, 2012; Hirabayashi et al., 2013) can be expected. To assess the impact of climate change on regional groundwater resources large-scale simulation models are necessary. Additionally, we expect the future variability of climate to be beyond that reflected in historical observations, which means that model predictions derive credibility via more in-depth diagnostic evaluation of the consistency between the model and the underlying system and not from some calibration exercise (Wagener et al., 2010).

Presently available global hydrology models discretise the land surface in grids with a resolution down to 0.25 to 0.5 decimal degrees. Parts of the vertical fluxes are well represented, e.g. the energy balance (Ek, 2003; Miralles et al., 2011). But groundwater recharge and groundwater flow are represented simply by heuristic equations (Döll and Fiedler, 2008a) or assumptions of linearity (Wada et al., 2010, 2014). They do not explicitly simulate a dynamic water table or regional groundwater flow. Global models also assume homogenous conditions of hydrologic and hydraulic properties in each of their grid cells, rather than variable flow paths, and they completely omit the possibility of preferential flow. This was criticized in the recent scientific discourse (Beven and Cloke, 2012; Wood et al., 2011).

The assumption of homogeneity is certainly inappropriate for karst regions. Chemical weathering of carbonate rock and other physical processes develop preferential pathways and strong subsurface heterogeneity (Bakalowicz, 2005). Flow and storage are heterogeneous ranging from very slow diffusion to rapid concentrated flow at the surface, in the soil, the unsaturated zone and the aquifer (Kiraly, 1998). A range of modeling studies have developed and applied karst specific models at individual karst systems at the catchment or aquifer scale (Doummar et al., 2012; Fleury et al., 2007; Hartmann et al., 2013b; Le Moine et al., 2008) but a lack of a priori information of

Simulation of groundwater recharge over Europe's karst regions

A. Hartmann et al.

[Title Page](#)

[Abstract](#)

[Introduction](#)

[Conclusions](#)

[References](#)

[Tables](#)

[Figures](#)

◀

▶

◀

▶

[Back](#)

[Close](#)

[Full Screen / Esc](#)

[Printer-friendly Version](#)

[Interactive Discussion](#)



Compared to the limited information about the deeper subsurface there is much better information about the surface and shallow subsurface including maps of soil types and properties (FAO/IIASA/ISRIC/ISSCAS/JRCv, 2012), observations of soil moisture (International Soil Moisture Network, Dorigo et al., 2011) and of latent heat fluxes (FluxNet, Baldocchi et al., 2001), and river discharge (GRDC, 2004). Surface and shallow subsurface information is used for the parameterization and evaluation of the surface routines of present large-scale models. But, although these data also cover Europe's karst regions, it has not been used for the development of large-scale models to simulate karstic surface and shallow subsurface flow and storage dynamics.

The objective of this study is to develop the first large-scale simulation model for groundwater recharge in Europe's karst regions. Despite much broader definitions of groundwater recharge (e.g., Lerner et al., 1990), we focus on vertical recharge, that is vertical percolation from the soil below the depth affected by evapotranspiration. We use a novel type of model structure that considers the sub-grid heterogeneity of karst properties using statistical distribution functions. To achieve a realistic parameterization of the model we identify typical karst landscapes by cluster analysis and by a combined use of a priori information about soil storage capacities and observations of recharge related fluxes and storage dynamics. Applying a parameter confinement strategy based on Monte Carlo sampling we are able to provide simulations of annual recharge over Europe's karst regions including a quantification of their uncertainty.

2 Data and methods

2.1 The model

Due to chemical weathering (karstification) karst systems have a strong subsurface heterogeneity of flow and storage processes (Bakalowicz, 2005) that have to be

Simulation of groundwater recharge over Europe's karst regions

A. Hartmann et al.

Title Page

Abstract

Introduction

Conclusions

References

Tables

Figures



Back

Close

Full Screen / Esc

Interactive Discussion



Simulation of groundwater recharge over Europe's karst regions

A. Hartmann et al.

[Title Page](#)

[Abstract](#)

[Introduction](#)

[Conclusions](#)

[References](#)

[Tables](#)

[Figures](#)

[◀](#)

[▶](#)

[◀](#)

[▶](#)

[Back](#)

[Close](#)

[Full Screen / Esc](#)

[Printer-friendly Version](#)

[Interactive Discussion](#)

considered to produce realistic simulations (Hartmann et al., 2014a). In this study, large-scale karst recharge is estimated by a modified version of the VarKarst model (Hartmann et al., 2013a), called VarKarst-R from here, on a 0.25×0.25 decimal degree grid. The model has shown to be applicable at various scales and climates over Europe (Hartmann et al., 2013b). Its main advantage includes the capability to represent subsurface heterogeneity using statistical distribution functions allowing for variable soil depths, variable epikarst depths and variable subsurface dynamics (Fig. 1). This leads to a parametrically efficient process representation. Comparisons with independently derived field data showed that these distribution functions are a good approximation of the natural heterogeneity (Hartmann et al., 2014c).

Heterogeneity of soil depths is represented by a mean soil storage capacity V_{soil} [mm] and a distribution coefficient a [–]. The soil storage capacity $V_{S,i}$ [mm] for every compartment i is defined by:

$$V_{S,i} = V_{\max,S} \cdot \left(\frac{i}{N} \right)^a \quad (1)$$

where $V_{\max,S}$ [mm] is the maximum soil storage capacity and N is the total number of model compartments. This is derived from the mean soil storage capacity V_{soil} as

$$\int_0^{i_{1/2}} V_{\max,S} \left(\frac{x}{N} \right)^a dx = \frac{\int_0^N V_{\max,S} \left(\frac{x}{N} \right)^a dx}{2}; V_{\text{soil}} = V_{\max,S} \left(\frac{i_{1/2}}{N} \right)^a \quad (2)$$

⇓

$$V_{\max,S} = V_{\text{soil}} \cdot 2^{\left(\frac{a}{a+1} \right)}$$

where $i_{1/2}$ is the compartment at which the soil storage capacities on the left equal the soil storage capacities on the right (Fig. 1a). Preceding work (Hartmann et al., 2013a, b) showed that the same distribution coefficient a can be used to derive the epikarst

storage distribution $V_{E,i}$ from the mean epikarst storage capacity V_{epi} [mm] (via the maximum epikarst storage $V_{\text{max},E}$ likewise to $V_{\text{max},S}$ in Eq. 2):

$$V_{E,i} = V_{\text{max},E} \cdot \left(\frac{i}{N} \right)^a \quad (3)$$

At each time step t , the actual evapotranspiration from each soil compartment $E_{\text{act},i}$ is found by:

$$E_{\text{act},i}(t) = E_{\text{pot}}(t) \cdot \frac{\min [V_{\text{Soil},i}(t) + P_{\text{eff}}(t) + Q_{\text{Surface},i}(t), V_{S,i}]}{V_{S,i}} \quad (4)$$

where E_{pot} [mm] is the potential evapotranspiration derived by the Priestley–Taylor equation (Priestley and Taylor, 1972), P_{eff} [mm] is the sum of liquid precipitation and snow melt, $Q_{\text{Surface},i}$ [mm] is the surface inflow arriving from compartment $i - 1$ (see

Eq. 9), and $V_{S,i}$ [mm] the water stored in the soil at time step t . Snow fall and snow melt are derived from daily snow water equivalent available from GLDAS-2 (Table 1). During days with snow cover we set $E_{\text{act}}(t) = 0$. Flow from the soil to the epikarst $R_{\text{Epi},i}$ [mm] is calculated by:

$$R_{\text{Epi},i}(t) = \max [V_{\text{Soil},i}(t) + P_{\text{eff}}(t) + Q_{\text{Surface},i}(t) - E_{\text{act},i}(t) - V_{S,i}, 0] \quad (5)$$

Following an assumption of linearity (Rimmer and Hartmann, 2012), the epikarst storage coefficients $K_{E,i}$ [d] controls the epikarst outflow dynamics:

$$Q_{\text{Epi},i}(t) = \frac{\min [V_{\text{Epi},i}(t) + R_{\text{Epi},i}(t), V_{E,i}]}{K_{E,i}} \cdot \Delta t \quad (6)$$

$$K_{E,i} = K_{\text{max},E} \cdot \left(\frac{N - i + 1}{N} \right)^a \quad (7)$$

[Title Page](#)

[Abstract](#)

[Introduction](#)

[Conclusions](#)

[References](#)

[Tables](#)

[Figures](#)

◀

▶

◀

▶

[Back](#)

[Close](#)

[Full Screen / Esc](#)

[Printer-friendly Version](#)

[Interactive Discussion](#)

where $V_{E,i}$ [mm] is the water stored in compartment i of the epikarst at time step t . Again, the same distribution coefficient a is applied to derive $K_{E,i}$ from $K_{\max,E}$. The latter is obtained from the mean epikarst storage coefficient K_{epi} using:

$$N \cdot K_{\text{mean},E} = \int_0^N K_{\max,E} \left(\frac{x}{N} \right)^a dx \quad (8)$$

\Updownarrow

$$K_{\max,E} = K_{\text{epi}} \cdot (a + 1)$$

- 5 When infiltration exceeds the soil and epikarst storage capacities, surface flow to the next model compartment $Q_{\text{Surf},i+1}$ [mm] initiates:

$$Q_{\text{Surf},i+1}(t) = \max [V_{\text{Epi},i}(t) + R_{\text{Epi},i}(t) - V_{E,i}, 0] \quad (9)$$

To summarize, the model is completely defined by the four parameters a , K_{epi} , V_{soil} , and V_{epi} .

10 2.2 Data availability

Forcing for the VarKarst-R model is derived through the Global Land Data Assimilation System (GLDAS-2) that assimilates satellite- and ground-based observational data products to obtain optimal fields of land surface states and fluxes (Rodell et al., 2004; Rui and Beaudoin, 2013). While precipitation, temperature and net radiation are

15 mainly merged from satellite and gauge observations, snow water equivalent is derived using data assimilation as well as the snow water equivalent simulations of the NOAH land surface model v3.3 (Ek, 2003) driven by GLDAS-2 forcing. Europe's carbonate rock areas are derived from a global map (vector data) of carbonate rock (Williams and Ford, 2006). Each cell of the 0.25 decimal degree simulation grid intersecting a carbonate rock region was considered a karst region. The model was calibrated and evaluated

[Title Page](#)

[Abstract](#)

[Introduction](#)

[Conclusions](#)

[References](#)

[Tables](#)

[Figures](#)

[◀](#)

[▶](#)

[◀](#)

[▶](#)

[Back](#)

[Close](#)

[Full Screen / Esc](#)

[Printer-friendly Version](#)

[Interactive Discussion](#)

Simulation of groundwater recharge over Europe's karst regions

A. Hartmann et al.

| | |
|------------------------------------------|------------------------------|
| Title Page | |
| Abstract | Introduction |
| Conclusions | References |
| Tables | Figures |
| ◀ | ▶ |
| ◀ | ▶ |
| Back | Close |
| Full Screen / Esc | |
| Printer-friendly Version | |
| Interactive Discussion | |

with observations of actual evapotranspiration from FLUXNET (Baldocchi et al., 2001) and with soil water content data from the International Soil Moisture Network ISMN (Dorigo et al., 2011). Only stations within carbonate rock regions and with ≥ 12 months of available data were used (Fig. 2). Months with < 25 days of observations were discarded. In addition, months with $\geq 50\%$ mismatch in their energy closure were discarded from the FLUXNET data set (similar to Miralles et al., 2011).

2.3 Parameter estimation

A lack of a priori information and observations of discharge and groundwater levels that can be used for calibration are the primary reasons why karst models have not been applied on larger scales yet (Hartmann et al., 2014a). The parameter assessment strategy we present in the following is meant to overcome this problem by using a combination of a priori information and recharge-related variables. We define typical karst landscapes over Europe and apply this combined information to a large initial sample of possible model parameter sets. In a step-wise process we then discard all parameter sets that produce simulations inconsistent with our a priori information and our recharge-related observations.

2.3.1 Definition of typical karst landscapes

Our definition of typical karst landscapes is based on the well-known hydrologic landscape concept (Winter, 2001), which describes hydrological landscapes based on their geology, relief and climate. Constraining ourselves to karst regions that mainly develop on carbonate rock we assume that differences among the karst landscapes are due to differences in relief and climate, and the consequent processes of landscape evolution including the weathering of carbonate rock (karstification). Europe's carbonate rock regions are divided into typical landscapes using simple descriptors of relief (range of altitude) and climate (aridity index and mean annual number of days with snow cover) within each of 0.25 decimal degree grid cells and a standard

clusteranalysis scheme (k-means method). We test the quality of clustering for 2 to 20 clusters by calculating the sums of squared internal distances to the cluster means. The so-called “elbow method” identifies the point where adding additional clusters only leads to a marginal reduction in the internal distance metric, i.e. the percentage of variance explained by adding more clusters would not increase significantly (Seber, 2009).

2.3.2 Model parameters for each karst landscape

We initially sample 25 000 possible model parameter sets from independent uniform distributions using parameter ranges derived from previous catchment scale applications of the VarKarst-R model over Europe (Table 2). We use a priori information and recharge-related observations to assess parameter performance for each karst landscape. A priori information consists of spatially distributed information about mean soil storage capacities as provided by several preceding mapping and modelling studies (Ek, 2003; FAO/IIASA/ISRIC/ISSCAS/JRCv, 2012; Miralles et al., 2011). Recharge-related variables are (1) soil moisture observations and (2) observations of actual evaporation at various locations over Europe (Table 1, Fig. 2). Soil moisture is related to recharge because it indicates the start and duration of saturation of the soil during which diffuse and preferential recharge can take place. Actual evaporation is related to recharge because usually no surface runoff occurs in karst regions due to the high infiltration capacities (Jeannin and Grasso, 1997). The difference of monthly precipitation and actual evaporation is therefore a valid proxy for groundwater recharge at a monthly time scale or above. The new parameter confinement strategy is applied to each of the karst landscapes in 3 steps:

1. Bias rule: retain only the parameter sets that produce a bias between observed and simulated actual evaporation lower than 75 % at all FLUXNET locations within

[Title Page](#)[Abstract](#)[Introduction](#)[Conclusions](#)[References](#)[Tables](#)[Figures](#)[◀](#)[▶](#)[◀](#)[▶](#)[Back](#)[Close](#)[Full Screen / Esc](#)[Printer-friendly Version](#)[Interactive Discussion](#)

Simulation of groundwater recharge over Europe's karst regions

A. Hartmann et al.

[Title Page](#)

[Abstract](#)

[Introduction](#)

[Conclusions](#)

[References](#)

[Tables](#)

[Figures](#)

◀

▶

◀

▶

[Back](#)

[Close](#)

[Full Screen / Esc](#)

[Printer-friendly Version](#)

[Interactive Discussion](#)



the chosen karst landscape:

$$\min_i(\text{bias}_i) = \min_i \left(\frac{\mu_{\text{sim},i} - \mu_{\text{obs},i}}{\mu_{\text{obs},i}} \right) < 75\% \quad (10)$$

Where $m_{\text{sim},i}$ and $m_{\text{obs},i}$ are the sum of simulated and observed actual evapotranspiration at location i , respectively. The value 75 % was found by trial-and-error reducing the initial sample to a reasonable number. The bias rule was not applied on the soil moisture since porosities of the soil matrix were not available prohibiting a comparison of simulated and observed soil water contents.

2. Correlation rule: retain only the parameter sets that produce a positive coefficient of (Pearson) correlation between observations and simulations of both actual evaporation and soil moisture, at all locations:

$$\left(\min_i [\text{corr}(\text{AET}_{\text{sim},i}, \text{AET}_{\text{obs},i})] \wedge \min_j [\text{corr}(\theta_{\text{sim},j}, \theta_{\text{obs},j})] \right) > 0 \quad (11)$$

where $\text{AET}_{\text{sim},j}$ and $\text{AET}_{\text{obs},j}$, and $\theta_{\text{sim},j}$ and $\theta_{\text{obs},j}$ are the monthly means of simulated and observed actual evapotranspiration, and soil water content at locations i/j , respectively.

3. Application of a priori information: retain only parameter sets in which V_{soil} falls within the feasible ranges that can be derived from a priori information about the maximum soil storage capacity in different karst landscapes (Ek, 2003; FAO/IIASA/ISRIC/ISSCAS/JRCv, 2012; Miralles et al., 2011). We add the a priori information at the last step to evaluate if the posterior distributions of V_{soil} already adapt to the ranges defined in this step. If they do not we would conclude that the recharge related information applied in confinement steps 1 and 2 is biased.

Each step reduces the initial parameter sample differently for each of the karst landscapes. The posterior parameter distributions within the confined samples should be different among the karst landscapes if the karst landscapes are properly defined.

Recharge is simulated over the carbonate regions of Europe from 2002/03 to 2011/12 using the confined parameter samples for each of the identified karst landscapes and the available forcings (Table 1). The mean and SD of simulated recharge for each grid cell and time step is calculated by uniform discrete sampling of a representative subset of 250 parameter sets from each of the confined parameters sets.

2.5 Model evaluation

To assess the realism of simulated groundwater recharge we compare simulated with observed mean annual recharge volumes derived independently from karst studies over Europe (Table 3). In addition, we compare our results to the simulated mean annual recharge volumes of two well-established global simulation models: PCR-GLOBWB (Wada et al., 2010, 2014) and WaterGAP (Döll and Fiedler, 2008a; Döll et al., 2003).

We furthermore apply a global sensitivity analysis strategy, called Regional Sensitivity Analysis (Spear and Hornberger, 1980), to evaluate the importance of the 4 model parameters at different simulation time scales ranging from 1 month up to 10 years. This analysis shows (1) which simulated process and characteristics are dominant at a given time scale and (2) which parameters will need more careful calibration when the model will be used in future studies. We use the same sample of 25 000 parameter sets that was created for the parameter estimation strategy (Sect. 2.3.2) and assess the sensitivity of 4 model outputs representative of different time scales: coefficient of variation (CV) of simulated monthly recharge volumes (monthly), CV of simulated 3-monthly recharge volumes (seasonal), CV of annual recharge volumes (annual), and total recharge over the entire 10 year simulation period (decadal). We do not consider temporal resolution less than a month given the assumption that the difference of precipitation and actual evapotranspiration can be a proxy for groundwater recharge,

Simulation of groundwater recharge over Europe's karst regions

A. Hartmann et al.

Title Page

Abstract

Introduction

Conclusions

References

Tables

Figures

Tables

Figures

Tables

Figures

Tables

Figures

Tables

Figures

1

1

1

1

Back

[Close](#)

Full Screen / Esc

Point of Sale Management

© 2010 by the Regents of the University of California



For each of the identified karst landscapes we choose the 10 locations that are closest to their cluster means (Euclidean distances to relief and climate descriptors;

- 5 Sect. 2.3.1) as representative locations. In the regional sensitivity analysis approach,
 we split the parameter sets into two groups, those that produce simulations above the
 simulated median of one of the 4 model outputs and those that produce simulations
 below. We then calculate the maximum distance $D(x)$ between marginal cumulative
 distribution functions (CDFs) produced by these two distributions for each of the param-
 eters – a large distance $D(x)$ suggests that the parameter is important for simulating
 10 this particular output (Fig. 3).

3 Results

3.1 Parameter assessment

3.1.1 Definition of typical karst landscapes

- 15 Cluster analysis resulted in four clusters, which are generally spatially contiguous (Fig. 4) and have quantitatively distinct cluster means (Table 4). We can attribute particular characteristics to each cluster using the mean values of the clustering descriptors (Table 4): (1) humid hills and plains (HUM) are characterised by an aridity index < 1, a significant number of days with snow cover and low elevation differences. (2)
20 High range mountains (MTN) have an aridity index of ~ 1, they also have a significant number of days with snow cover and they show very large topographic elevation differences. (3) Mediterranean medium range mountains show a high aridity index, only few days with snow cover and high elevation differences. (4) Desert hills and plains are described by similar altitude ranges as the humid hills and plains but they have a high aridity indices and almost no days with snow cover. The karst landscapes order
25



from North (HUM) to South (DES) based on increasing temperatures and decreasing precipitation amounts. While HUM and DES appear to be separated clearly, MTN and MED mix in some regions, for instance Greece and Turkey.

3.1.2 Model parameter estimates for each karst landscape

- 5 The three steps of the new parameter confinement strategy resulted in a significant re-
duction of the initial sample of 25 000 parameter sets (Fig. 5). Each step has a different
impact on the reduction among the identified landscapes. For the humid karst land-
scapes, the correlation rule appears to have the strongest impact while for the moun-
tain and Mediterranean landscapes the bias rule results in the strongest reduction. For
10 the desert landscape only step 3, i.e. application of a priori information, reduces the
initial sample because no data was available to apply steps 1 and 2. Considering the
parameter ranges for each landscape after the application of the confinement strat-
egy (Table 5), we only achieved a confinement of the distribution parameter a , the soil
storage capacity V_{soil} , and slight confinement of the epikarst storage coefficient K_{epi} .

15 The impact of the three confinement steps becomes more obvious when considering
 their posterior distributions (Fig. 6). The distributions of parameters a , K_{epi} and V_{soil}
 evolve significantly away from their initial uniform distributions along the confinement
 steps. In general, changes of the posterior distributions of each landscape's parameter
 samples are in accordance with the reductions of their number (Fig. 5), though changes
 20 are pronounced differently among the parameters. While a and V_{soil} change strongly for
 HUM, MTN and MED, V_{epi} maintains a uniform distribution across all steps. K_{epi} also
 exhibits strong changes for HUM but they are less pronounced for MTN and MED. The
 posterior distributions of the DES landscape do not change except for step 3 due to
 the lack of information to apply confinement steps 1 and 2. Step 3 results in a tailoring
 25 of the distribution of V_{soil} for all landscapes. For HUM, MTN and MED it can be seen
 that confinement steps 1 and 2 already pushed the parameter distributions towards
 their final shape, meaning that the changes in parameter distributions induced by the

Simulation of groundwater recharge over Europe's karst regions

A. Hartmann et al.

Title Page

Abstract

Introduction

Conclusions

References

Tables

Figures

Tables

Figures

Tables

1

▶

1

Back

Close

Full Screen / Esc

Printer friendly Version

Interactive Discussion



comparison with observations are consistent with the a priori information about the physical characteristics of the karst.

3.2 Recharge simulations over Europe

The parameter confinement strategy allows us to apply VarKarst-R over all of Europe and to obtain recharge simulations for the hydrological years 2002/03–2011/12. Thanks to the 250 parameter sets that we samples from the posterior parameter distributions we can include an estimate of uncertainty for each grid cell (Fig. 7). Mean annual recharge ranges from almost 0 to $> 1000 \text{ mm a}^{-1}$ with the highest volumes found in Northern England, the Alps and former Yugoslavia. The lowest values are found in the desert regions of Northern Africa. The vast majority of recharge rates ranges from 20–50 % of precipitation. Considering the simulations individually for each karst landscape reveals that the mountain landscapes produce the largest recharge volumes followed by the humid and Mediterranean landscapes (Fig. 8a). The desert landscapes produce the lowest recharge volumes. However, the recharge rates reveal that on average the Mediterranean landscapes show the largest recharge rates, followed by the highly variable mountains (Fig. 8c). Humid and deserts landscapes exhibit lower recharge rates. Uncertainties, expressed by the SD of the 250 simulations for each grid cell, are rather low, seldom exceeding 35 mm a^{-1} (Fig. 8b). However, expressed as coefficients of variation, most of them range from 5–25 % for the humid, mountain and Mediterranean landscapes but for the desert landscape they can reach up to 50 % of the mean annual recharge (Fig. 8d).

3.3 Model evaluation

We compare the simulated recharge volumes of our model with recharge volumes assessed from independent and published karst studies over Europe (Fig. 9a). Even though there is a considerable spread across the simulations their bulk plots well around the 1 : 1 line achieving an average deviation of only -22 mm a^{-1} (Table 6).

[Title Page](#)[Abstract](#)[Introduction](#)[Conclusions](#)[References](#)[Tables](#)[Figures](#)[◀](#)[▶](#)[◀](#)[▶](#)[Back](#)[Close](#)[Full Screen / Esc](#)[Printer-friendly Version](#)[Interactive Discussion](#)

Considering the individual karst landscapes there is an over-estimation of recharge for the humid landscapes and an under-estimation for the mountain landscapes. The best results are achieved for the Mediterranean landscapes with only slight under-estimation (Fig. 9a). When we compare the same observations to the simulated recharge volumes of the PCR-GLOBWB (Fig. 9b) and WaterGAP models (Fig. 9c) we find a strong tendency of under-estimation that is strongest for the mountain and Mediterranean landscapes but still significant for the humid landscapes (Table 6). For the humid landscapes absolute deviations are similar among the three models.

In addition to comparing simulated and observed annual averages, sensitivity analysis on the model output gives us insight in the realism of the model and the importance of individual model parameters at different time scales (Fig. 10). Our results show that parameters a and V_{soil} have the overall strongest influence on the simulated recharge from a monthly to a 10 year time scale but their influence decreases toward shorter time scales. Simultaneously the epikarst parameter K_{epi} gains more importance. This behaviour is most pronounced for the Mediterranean and desert landscapes. The same is true for V_{epi} , but its overall importance remains much lower, which was also found in the parameter confinement strategy (Fig. 6).

4 Discussion

4.1 Reliability of parameter estimation

4.1.1 Identification of karst landscapes

The identification of different karst landscapes is a crucial step within our new parameter estimation strategy. The four karst landscapes we identified depend mostly on the choice of climatic and topographic descriptors (Table 4) and the selected number of clusters. The choice of descriptors is well justified from our understanding of hydrologic process controls as formalized in the hydrologic landscape concept (Winter, 2001)

Simulation of groundwater recharge over Europe's karst regions

A. Hartmann et al.

[Title Page](#)

[Abstract](#)

[Introduction](#)

[Conclusions](#)

[References](#)

[Tables](#)

[Figures](#)

◀

▶

◀

▶

[Back](#)

[Close](#)

[Full Screen / Esc](#)

[Printer-friendly Version](#)

[Interactive Discussion](#)



and applied similarly at many other studies (Leibowitz et al., 2014; Sawicz et al., 2011; Wigington et al., 2013). The appropriate choice of clusters for the k means method is less unambiguous (Ketchen and Shook, 1996). The change in number of clusters when the sum of squared distances to our cluster centres only reduces marginally was not clearly definable (Fig. A1). However, choosing only 3 clusters instead of 4 would have resulted in unrealistic spatial distribution of clusters. The attribution of Northern African regions with Northern Europe to the same cluster occurred because of their similarity of altitude ranges (Table 4). On the other hand, a selection of 5 clusters would have resulted in a cluster with properties just between the MTN and the MED clusters and, because of a much stronger scattering, weaker spatial distinction between them. With 4 clusters our karst landscapes are similar to the Koeppen Geiger climate regions (Kottek et al., 2006), in particular the Oceanic Climate (HUM), the Hot and Warm summer Mediterranean Climate (MED), and the Hot Desert Climates (DES). We see deviations when comparing the Polar and Alpine Climate regions of Koeppen–Geiger with our High Range Mountain karst landscape though, since our landscapes are also defined by their elevation ranges.

The borders of these hydrologic landscapes are also uncertain. Natural systems usually do not have as straight borders that fall on a grid as assumed by this analysis. Transitions between landscape types are rather continuous and hence transitions from a parameter set representing one landscape to another parameter set of another cluster should be transient, as well. This will be discussed in the following subsection.

4.1.2 Confinement of parameters

How the 3 steps of the parameter confinement strategy reduce the initial sample shows which type of data provides the most relevant information for each of the karst landscapes. While the timing of actual evapotranspiration and soil saturation that is expressed by the correlation rule appears to be most relevant for the humid landscapes, the bias rule, which represents the volumes of monthly evapotranspiration is more relevant for the mountain and Mediterranean landscapes. Swapping the correlation rule

Simulation of groundwater recharge over Europe's karst regions

A. Hartmann et al.

[Title Page](#)

[Abstract](#)

[Introduction](#)

[Conclusions](#)

[References](#)

[Tables](#)

[Figures](#)

[◀](#)

[▶](#)

[◀](#)

[▶](#)

[Back](#)

[Close](#)

[Full Screen / Esc](#)

[Printer-friendly Version](#)

[Interactive Discussion](#)



and the bias rule in their order would provide the same results for HUM and MTN. But for MED the other order increases the importance of timing expressed by the correlation rule indicating similar importance of both confinement steps.

The thresholds we set in confinement step 1 and 2 are not very strict, and the ranges of soil storage capacity we used as a priori information in step 3 are quite large. This compensates for the fact that (1) only recharge-related variables are available rather than direct recharge observations, (2) these variables are not available at the simulation scale (0.25° grid) but at a point-scale, and (3) the transition between the landscapes is more continuous than discrete. Despite these rather weak constraints, the initial parameter sample of 25 000 reduces to a quite low numbers between 679 (HUM) and 2731 (MED). All posterior parameters overlap except for the soil storage capacities that are tailored by the a priori information (confinement step 3). Hence, a little number of parameter sets for one landscape is also acceptable for some of the other landscape and therefore taking into account the continuous transition between them.

All model parameters, except for V_{epi} , show different shapes in their cumulative distribution functions across the karst landscapes. The desert landscape parameters only differ from the initial sample for the V_{soil} parameter due to the lack of information to apply confinement steps 1 and 2. The distribution parameter a is found at the lower values of its feasible range for the humid and mountain landscapes indicating a significant contribution of preferential recharge. Since altitude ranges are rather low for HUM this may be attributed to a significant epikarst development (Perrin et al., 2003; Williams, 1983). For MTN a mixture of epikarst development and topography driven interflow at the mountain hill slopes and valleys can be expected to control the dynamics of karstic recharge (Scanlon et al., 2002; Tague and Grant, 2009). At the Mediterranean landscapes the a parameter adapts to ranges that are rather found at the higher values of its initial range indicating that there is a stronger differentiation between diffuse and concentrated recharge. This may be due to the generally thinner soils (Table 5) that limit the availability of CO_2 for karst evolution (Ford and Williams, 2007). Instead, local surface runoff channels the water to the next enlarged fissure or crack to reach the

Simulation of groundwater recharge over Europe's karst regions

A. Hartmann et al.

[Title Page](#)[Abstract](#)[Introduction](#)[Conclusions](#)[References](#)[Tables](#)[Figures](#)[◀](#)[▶](#)[◀](#)[▶](#)[Back](#)[Close](#)[Full Screen / Esc](#)[Printer-friendly Version](#)[Interactive Discussion](#)

subsurface as concentrated recharge (Lange et al., 2003). The epikarst storage coefficient K_{epi} for HUM and MED is at lower values of the initial range indicating realistic mean residence times of days to weeks (Aquilina et al., 2006; Hartmann et al., 2013a). The MTN landscapes show larger K_{epi} values indicating slower epikarst dynamics most probably due to the reasons mentioned above. The application of a priori information in confinement step 3 automatically tailors the values of V_{soil} to ranges that we assume to be realistic. The fact that confinement steps 1 and 2 already push the shape of their posteriors towards the a priori ranges corroborates that assumption.

The little changes that occur to the initial distributions of the DES parameter sets elaborate the flexibility of our parameter assessment strategy. The posterior distribution evolves only where information is available (for this landscape on V_{soil}). This is also evident in the behaviour of parameter V_{epi} . The available information is just not precise enough to achieve identification beyond its a priori ranges. For parameter a in HUM, MTN and MED, a lot of information is derived from the available data and its posteriors differ strongly from its initial distribution, while there is less information to determine K_{epi} . This explicit handling of uncertainties in the parameter identification process allows us to provide recharge simulations over Europe's karst regions with uncertainty estimates that represent confidence for each of the identified karst landscapes.

4.2 Simulation of karst recharge over Europe

4.2.1 Realism of spatial patterns

Simulated mean annual recharge volumes for the period 2002/03–2011/12 show a wide range of values, from $0 > 1000 \text{ mm a}^{-1}$ (Fig. 7). Total water availability (mean annual precipitation) appears to be the main driver for its spatial pattern in many regions, for instance at former Yugoslavia or Northern UK. This is consistent with findings of other studies (Hartmann et al., 2014c; Samuels et al., 2010). When we normalize the recharge rates by the observed precipitation amounts we find that water availability is not the only control on mean annual recharge volumes. A strong relation of

Simulation of groundwater recharge over Europe's karst regions

A. Hartmann et al.

[Title Page](#)

[Abstract](#)

[Introduction](#)

[Conclusions](#)

[References](#)

[Tables](#)

[Figures](#)

◀

▶

◀

▶

[Back](#)

[Close](#)

[Full Screen / Esc](#)

[Printer-friendly Version](#)

[Interactive Discussion](#)

Simulation of groundwater recharge over Europe's karst regions

A. Hartmann et al.

[Title Page](#)

[Abstract](#)

[Introduction](#)

[Conclusions](#)

[References](#)

[Tables](#)

[Figures](#)

[◀](#)

[▶](#)

[◀](#)

[▶](#)

[Back](#)

[Close](#)

[Full Screen / Esc](#)

[Printer-friendly Version](#)

[Interactive Discussion](#)

evapotranspiration and karst characteristics and processes was shown in many studies and is also found here (Heilman et al., 2014; Jukic and Denic-Jukic, 2008). Potential evaporation is generally increasing from North to South and has an important impact on recharge rates as well; for instance on the Arabian Peninsula or in the Alps.

5 Mountain ranges are considered to be the water towers of the world (Viviroli et al., 2007). Here the MTN landscapes also show the largest recharge volumes due to the large precipitation volumes they receive, though with a considerable spread in our study. HUM and MED landscapes behave similarly with significantly less recharge than MTN. Not surprisingly there is not much recharge in the desert landscapes at all. But 10 the differences among the clusters shift when considering recharge rates. Due to their thin soils, and therefore low soil storage for evaporation (Table 5), the DES karst landscapes transfer up to 45 % of the little precipitation they receive into recharge. The MED landscapes show similarly high recharge rates. Though since their soils are generally thicker than the DES soils the typical seasonal and convective rainfall patterns of 15 the Mediterranean climate (Goldreich, 2003; Lionello, 2012) might have an important impact, too.

Even though there is still considerable spread in our confined parameter sets, the uncertainty in simulated mean annual recharge volumes is quite low. The uncertainties that follow the limited information content of the observations are revealed more clearly 20 when we relate the SD of simulated recharge to its mean volumes with the coefficient of variation. The uncertainty for the DES landscape is the largest among the clusters because a priori information is only available for V_{soil} . The uncertainty reduces for the MED and MTN landscapes. The low uncertainties for the coefficient of variation of our recharge simulations for the HUM landscape indicate that the available data contained 25 significant information for confining the model parameter ranges.

4.2.2 Relevance of different recharge processes to simulation time scales

The mean annual water balance of a hydrological system is dominated by the separation of precipitation into actual evapotranspiration and discharge (Budyko and Miller,

1974; Sivapalan et al., 2011). Actual evapotranspiration is controlled by the soil storage capacity V_{soil} and the distribution coefficient a within the VarKarst-R model. Regional sensitivity analysis shows that both of them are most sensitive for the 10 year and annual time scale (Fig. 10). Both parameters loose some impact at higher temporal resolutions (seasonal or monthly time scale) in favour of the parameters that control the dynamics of the epikarst. This behaviour is consistent with evidence from field and other modelling studies that showed that the epikarst can be considered as a temporary storage and distribution system for karstic recharge (Hartmann et al., 2012; Williams, 1983) – potentially storing water for several days to weeks (Aquilina et al., 2006; Hartmann et al., 2013a). Parameter V_{epi} does not show much sensitivity across all landscapes as suggested by the posterior distributions of the confinement strategy. First of all, this finding indicates that the data we used for our confinement strategy do not bias the general model behaviour. It also shows that for the epikarst storage and flow dynamics K_{epi} is much more important when simulating at monthly or seasonal resolution.

Furthermore, the results of the regional sensitivity analysis show which parameters are most important at a given time scale. Depending on the purpose a new study may start with the initial ranges of the model parameters or it might continue with the confined parameter ranges that we found here. The latter would result in slightly different sensitivities (Fig. A2). For both cases, the epikarst parameters will require more attention when applying the VarKarst-R model for simulations at seasonal or monthly time scales. When working at a smaller spatial scale, additional analysis of spring discharge and its hydrochemistry may provide such additional information (Lee and Krothe, 2001; Mudarra and Andreo, 2011). When working at a time scale of > 1 year the distribution parameter a and the soil storage capacity V_{soil} require most attention if one starts from the initial ranges. The distribution parameter is most important when using the confined ranges. Again, spring discharge analysis may help to understand the degree of karstification (Kiraly, 2003) and the distribution of concentrated and diffuse recharge mechanisms that are controlled by a . In addition, more precise digital elevation models

Simulation of groundwater recharge over Europe's karst regions

A. Hartmann et al.

[Title Page](#)

[Abstract](#)

[Introduction](#)

[Conclusions](#)

[References](#)

[Tables](#)

[Figures](#)

[◀](#)

[▶](#)

[◀](#)

[▶](#)

[Back](#)

[Close](#)

[Full Screen / Esc](#)

[Printer-friendly Version](#)

[Interactive Discussion](#)



or soil maps may help to better identify a and V_{soil} . A limitation of the regional sensitivity analysis approach used here is that parameter interactions are only included implicitly, considering parameter interactions with more elaborated methods (Saltelli et al., 2008) may reveal even more characteristics of the VarKarst-R model at different simulation time scales. But this is beyond the scope of this study.

4.3 Impact of karstic subsurface heterogeneity

Even though some deviations occur among the individual karst landscapes, the general simulations of the VarKarst-R model follow observations of mean annual recharge rates over Europe well (Fig. 9). On the other hand, the widely-used large-scale simulation models PCR-GLOBWB (Wada et al., 2010, 2014) and WaterGAP (Döll and Fiedler, 2008b; Döll et al., 2003) generally under-estimate groundwater recharge (Table 6). The reason for this is the representation of karstic subsurface heterogeneity within the VarKarst-R model, i.e. the inclusion of preferential flowpaths and of subsurface heterogeneity. Based on the conceptual understanding of soil and epikarst storage behaviour (Fig. 1c) it allows (1) for more recharge during wet conditions because surface runoff does not exist, and (2) for more recharge during dry conditions because the thin soil compartments will always allow for some water to percolate downwards before it is consumed by evapotranspiration. During wet conditions, both PCR-GLOBWB and WaterGAP would produce surface runoff instead that is therefore lost from groundwater recharge. During dry conditions, due to its non-variable soil storage capacity, the PCR-GLOBWB model would not produce any recharge when the soil water is below its minimum storage. Separating surface runoff and groundwater recharge by a constant factor the WaterGAP model would produce recharge during dry conditions, but a constant fraction of effective precipitation will always become fast surface/subsurface runoff resulting in reduced recharge volumes.

This does not mean that the representation of recharge processes in models like PCR-GLOBWB or WaterGAP is generally wrong, but can be limited since our analysis shows that the structures of such models need more adaption to the particularities

Simulation of groundwater recharge over Europe's karst regions

A. Hartmann et al.

[Title Page](#)

[Abstract](#)

[Introduction](#)

[Conclusions](#)

[References](#)

[Tables](#)

[Figures](#)

◀

▶

◀

▶

[Back](#)

[Close](#)

[Full Screen / Esc](#)

[Printer-friendly Version](#)

[Interactive Discussion](#)



Simulation of groundwater recharge over Europe's karst regions

A. Hartmann et al.

[Title Page](#)

[Abstract](#)

[Introduction](#)

[Conclusions](#)

[References](#)

[Tables](#)

[Figures](#)

◀

▶

◀

▶

[Back](#)

[Close](#)

[Full Screen / Esc](#)

[Printer-friendly Version](#)

[Interactive Discussion](#)



of different hydrologic landscapes. In particular it adds to the need for incorporating sub-grid heterogeneity in our large-scale simulation models (Beven and Cloke, 2012). Karst regions contribute about 35 % of Europe's land surface and our results indicate that presently their groundwater recharge is under-estimated, while surface runoff and actual evaporation are over-estimated. Given the expected decrease of precipitation in semi-arid regions, such as the Mediterranean, and an increase of extreme rainfall events at the same time in the near future (2016–2035, Kirtman et al., 2013) present large-scale simulation models will over-estimate both the vulnerability of groundwater recharge and the flood hazard in Europe's karst regions. The same is true for the long-term future (end of 21st century, Collins et al., 2013). Of course, an over-estimation of vulnerability and hazard might be the "lesser evil" compared to an over-estimation. But at times of limited financial resources excessive investments into drinking water and flood risk management for potential future changes may unnecessarily aggravate the socio-economic impacts of climate change.

5 Conclusions

In this study we presented the first attempt to model groundwater recharge over all karst regions in Europe. The model application was made possible by a novel parameter confinement strategy that utilized a combination of a priori information and recharge related observations on 4 typical karst landscapes that were identified through cluster analysis. Handling the remaining uncertainty explicitly as posterior parameter distributions resulting from the confinement strategy we were finally able to produce recharge simulations and an estimate of their uncertainty over Europe's karst regions. We found an adequate agreement with our new model when comparing our results with independent observations of recharge at study sites over Europe. We further show that present large-scale modelling approaches tend to significantly under-estimate recharge volumes.

Overall, our analysis showed that the subsurface heterogeneity of karst regions and the presence of preferential flowpaths enhances recharge. It results in high infiltration capacities prohibiting surface runoff and reducing actual evapotranspiration during wet conditions. On the other hand it allows for recharge during dry conditions because some water can always percolate downwards passing the thin fraction of the distributed soil depths. This particular behaviour suggests that karstic regions might be more resilient to climate change in terms of both flooding and droughts. Drinking water and flood risk management is prone to be based on erroneous information at least at the 35 % of Europe's land surface since this is not considered in current large-scale modelling approaches.

However, using recharge directly as a proxy for “available” groundwater resources may not be good in all cases, neither in karst regions nor in other types of aquifers (Bredehoeft, 2002). To precisely estimate the sustainably usable fraction of groundwater the aquifer outflow should be known rather than the inflow and pumping strategies should consider the geometry and transmissivity of the aquifer. Hence, recharge estimation can be considered only as a first proxy of available groundwater and future studies should focus on the large-scale simulation of karst groundwater flow and storage to further improve water resources predictions in karst regions.

Acknowledgements. We want to thank Juergen Strub from the Chair of Hydrology, Freiburg, Germany, for designing some of the figures and Thomas Godman for collecting references to independent recharge studies. This work was supported by a fellowship within the Postdoc Programme of the German Academic Exchange Service [Andreas Hartmann, DAAD] and by the UK Natural Environment Research Council [Francesca Pianosi, CREDIBLE Project; grant number NE/J017450/1]. We thank Petra Döll for providing the mean annual recharge volumes of WaterGAP, and Fanny Sarazin for checking the results of the regional sensitivity analysis.

Simulation of groundwater recharge over Europe's karst regions

A. Hartmann et al.

[Title Page](#)

[Abstract](#)

[Introduction](#)

[Conclusions](#)

[References](#)

[Tables](#)

[Figures](#)

[◀](#)

[▶](#)

[◀](#)

[▶](#)

[Back](#)

[Close](#)

[Full Screen / Esc](#)

[Printer-friendly Version](#)

[Interactive Discussion](#)

References

Simulation of groundwater recharge over Europe's karst regions

A. Hartmann et al.

[Title Page](#)

[Abstract](#)

[Introduction](#)

[Conclusions](#)

[References](#)

[Tables](#)

[Figures](#)

◀

▶

◀

▶

[Back](#)

[Close](#)

[Full Screen / Esc](#)

[Printer-friendly Version](#)

[Interactive Discussion](#)

- Allocca, V., Manna, F., and De Vita, P.: Estimating annual groundwater recharge coefficient for karst aquifers of the southern Apennines (Italy), *Hydrol. Earth Syst. Sci.*, 18, 803–817, doi:10.5194/hess-18-803-2014, 2014.
- 5 Andreo, B., Vías, J., Durán, J., Jiménez, P., López-Geta, J., and Carrasco, F.: Methodology for groundwater recharge assessment in carbonate aquifers: application to pilot sites in southern Spain, *Hydrogeol. J.*, 16, 911–925, doi:10.1007/s10040-008-0274-5, 2008.
- Aquilina, L., Ladouce, B., and Doerfliger, N.: Water storage and transfer in the epikarst of karstic systems during high flow periods, *J. Hydrol.*, 327, 472–485, 2006.
- 10 Arnell, N. W.: Relative effects of multi-decadal climatic variability and changes in the mean and variability of climate due to global warming: future streamflows in Britain, *J. Hydrol.*, 270, 195–213, 2003.
- Aydin, H., Ekmekci, M., and Soylu, M. E.: Characterization and conceptualization of a relict karst aquifer (bilecik, turkey) karakterizacija in konceptualizacija reliktnega, *Acta Carsologica*, 42, 75–92, 2013.
- 15 Bakalowicz, M.: Karst groundwater: a challenge for new resources, *Hydrogeol. J.*, 13, 148–160, 2005.
- Baldocchi, D., Falge, E., Gu, L., Olson, R., Hollinger, D., Running, S., Anthoni, P., Bernhofer, C., Davis, K., Evans, R., Fuentes, J., Goldstein, A., Katul, G., Law, B., Lee, X., Malhi, Y., Meyers, T., Munger, W., Oechel, W., Paw, K. T., Pilegaard, K., Schmid, H. P., Valentini, R., Verma, S., Vesala, T., Wilson, K., and Wofsy, S.: FLUXNET: a new tool to study the temporal and spatial variability of ecosystem-scale carbon dioxide, water vapor, and energy flux densities, *B. Am. Meteorol. Soc.*, 82, 2415–2434, doi:10.1175/1520-0477(2001)082<2415:fantts>2.3.co;2, 2001.
- 20 Barbieri, M., Boschetti, T., Petitta, M., and Tallini, M.: Stable isotope (^2H , ^{18}O and $^{87}\text{Sr}/^{86}\text{Sr}$) and hydrochemistry monitoring for groundwater hydrodynamics analysis in a karst aquifer (Gran Sasso, Central Italy), *Appl. Geochem.*, 20, 2063–2081, doi:10.1016/j.apgeochem.2005.07.008, 2005.
- 25 Beven, K. J. and Cloke, H. L.: Comment on “Hyperresolution global land surface modeling: Meeting a grand challenge for monitoring Earth’s terrestrial water” by Eric F. Wood et al., *Water Resour. Res.*, 48, W01801, doi:10.1029/2011WR010982, 2012.
- 30

- Bonacci, O.: Analysis of the maximum discharge of karst springs, *Hydrogeol. J.*, 9, 328–338, doi:10.1007/s100400100142, 2001.
- Bredehoeft, J. D.: The water budget myth revisited: why hydrogeologists model, *Ground Water*, 40, 340–345, 2002.
- 5 Budyko, D. H. and Miller, M. I.: Climate and Life, Academic Press, 1974.
- Christensen, J. H., Hewitson, B., Busuioc, A., Chen, A., Gao, X., Held, I., Jones, R., Kolli, R. K., Kwon, W.-T., Laprise, R., Rueda, V. M., Mearns, L., Menéndez, C. G., Räisänen, J., Rinke, A., Sarr, A., and Whetton, P.: Regional climate projections, in: Climate Change 2007: The Physical Science Basis, Contribution of Working Group I to the Fourth Assessment Report of the Intergovernmental Panel on Climate Change, edited by: Solomon, S., Qin, D., Manning, M., Chen, Z., Marquis, M., Averyt, K. B., Tignor, M., and Miller, H. L., Cambridge University Press, Cambridge, UK and New York, NY, USA, 996 pp., available at: http://www.ipcc.ch/publications_and_data/publications_ipcc_fourth_assessment_report_wg1_report_the_physical_science_basis.htm (last access: 17 November 2014), 2007.
- 10 15 Collins, M., Knutti, R., Arblaster, J. M., Dufresne, J.-L., Fichefet, T., Friedlingstein, P., Gao, X., Gutowski, W. J., Johns, T., and Krinner, G.: Long-term climate change: projections, commitments and irreversibility, in: Climate Change 2013: The Physical Science Basis, Contribution of Working Group I to the Fifth Assessment Report of the Intergovernmental Panel on Climate Change, edited by: Stocker, T. F., Qin, D., Plattner, G.-K., Tignor, M., Allen, S. K., Boschung, J., Nauels, A., Xia, Y., Bex, V., and Midgley, P. M., Cambridge University Press, Cambridge, UK and New York, NY, USA, 1029–1136, 2013.
- 20 COST: COST 65: Hydrogeological Aspects of Groundwater Protection in Karstic Areas, Final report (COST action 65), European Comission Dir. XII Sci. Res. Dev., Report EUR 16547 EN, 446 pp., 1995.
- 25 Dai, A.: Increasing drought under global warming in observations and models, *Nat. Clim. Chang.*, 3, 52–58, doi:10.1038/nclimate1633, 2012.
- Döll, P. and Fiedler, K.: Global-scale modeling of groundwater recharge, *Hydrol. Earth Syst. Sci.*, 12, 863–885, doi:10.5194/hess-12-863-2008, 2008.
- 30 Döll, P., Kaspar, F., and Lehner, B.: A global hydrological model for deriving water availability indicators: model tuning and validation, *J. Hydrol.*, 270, 105–134, doi:10.1016/S0022-1694(02)00283-4, 2003.
- Dorigo, W. A., Wagner, W., Hohensinn, R., Hahn, S., Paulik, C., Xaver, A., Gruber, A., Drusch, M., Mecklenburg, S., van Oevelen, P., Robock, A., and Jackson, T.: The International

Simulation of groundwater recharge over Europe's karst regions

A. Hartmann et al.

[Title Page](#)

[Abstract](#)

[Introduction](#)

[Conclusions](#)

[References](#)

[Tables](#)

[Figures](#)

◀

▶

◀

▶

[Back](#)

[Close](#)

[Full Screen / Esc](#)

[Printer-friendly Version](#)

[Interactive Discussion](#)



Soil Moisture Network: a data hosting facility for global in situ soil moisture measurements, *Hydrol. Earth Syst. Sci.*, 15, 1675–1698, doi:10.5194/hess-15-1675-2011, 2011.

Doummar, J., Sauter, M., and Geyer, T.: Simulation of flow processes in a large scale karst system with an integrated catchment model (Mike She) – Identification of relevant parameters influencing spring discharge, *J. Hydrol.*, 426–427, 112–123, doi:10.1016/j.jhydrol.2012.01.021, 2012.

Einsiedl, F.: Flow system dynamics and water storage of a fissured-porous karst aquifer characterized by artificial and environmental tracers, *J. Hydrol.*, 312, 312–321, 2005.

Ek, M. B.: Implementation of Noah land surface model advances in the National Centers for Environmental Prediction operational mesoscale Eta model, *J. Geophys. Res.*, 108, 12-1–12-16, doi:10.1029/2002jd003296, 2003.

Farr, T. G., Rosen, P. A., Caro, E., Crippen, R., Duren, R., Hensley, S., Kobrick, M., Paller, M., Rodriguez, E., Roth, L., Seal, D., Shaffer, S., Shimada, J., Umland, J., Werner, M., Oskin, M., Burbank, D., and Alsdorf, D.: The Shuttle Radar Topography Mission, (2005), 45, 1–33, doi:10.1029/2005RG000183, 2007.

FAO/IIASA/ISRIC/ISSCAS/JRCv: Harmonized World Soil Database (version 1.2), edited by: FAO/IIASA, 2012.

Fleury, P., Plagnes, V., and Bakalowicz, M.: Modelling of the functioning of karst aquifers with a reservoir model: application to Fontaine de Vaucluse (South of France), *J. Hydrol.*, 345, 38–49, 2007.

Ford, D. C. and Williams, P. W.: Karst Hydrogeology and Geomorphology, Wiley, Chichester, 2007.

Gleeson, T., Wada, Y., Bierkens, M. F., and van Beek, L. P.: Water balance of global aquifers revealed by groundwater footprint, *Nature*, 488, 197–200, doi:10.1038/nature11295, 2012.

Gleeson, T., Moosdorf, N., Hartmann, J., and van Beek, L. P. H.: A glimpse beneath earth's surface: GLobal HYdrogeology MaPS (GLHYMPS) of permeability and porosity, *Geophys. Res. Lett.*, 41, 3891–3898, doi:10.1002/2014GL059856, 2014.

Goldreich, Y.: The Climate of Israel: Observation, Research and Application, Kluwer Academic/Plenum Publishers, 2003.

GRDC: Long Term Mean Annual Freshwater Surface Water Fluxes into the World Oceans, Comparisons of GRDC Freshwater Flux Estimate With Literature, available at: <http://grdc.bafg.de/servlet/is/7083/> (last access: 17 November 2014), 2004.

Simulation of groundwater recharge over Europe's karst regions

A. Hartmann et al.

[Title Page](#)

[Abstract](#)

[Introduction](#)

[Conclusions](#)

[References](#)

[Tables](#)

[Figures](#)

◀

▶

◀

▶

[Back](#)

[Close](#)

[Full Screen / Esc](#)

[Printer-friendly Version](#)

[Interactive Discussion](#)



- Hartmann, A., Lange, J., Weiler, M., Arbel, Y., and Greenbaum, N.: A new approach to model the spatial and temporal variability of recharge to karst aquifers, *Hydrol. Earth Syst. Sci.*, 16, 2219–2231, doi:10.5194/hess-16-2219-2012, 2012.
- Hartmann, A., Barberá, J. A., Lange, J., Andreo, B., and Weiler, M.: Progress in the hydrologic simulation of time variant recharge areas of karst systems – Exemplified at a karst spring in Southern Spain, *Adv. Water Resour.*, 54, 149–160, doi:10.1016/j.advwatres.2013.01.010, 2013a.
- Hartmann, A., Weiler, M., Wagener, T., Lange, J., Kralik, M., Humer, F., Mizyed, N., Rimmer, A., Barberá, J. A., Andreo, B., Butscher, C., and Huggenberger, P.: Process-based karst modelling to relate hydrodynamic and hydrochemical characteristics to system properties, *Hydrol. Earth Syst. Sci.*, 17, 3305–3321, doi:10.5194/hess-17-3305-2013, 2013b.
- Hartmann, A., Goldscheider, N., Wagener, T., Lange, J., and Weiler, M.: Karst water resources in a changing world: review of hydrological modeling approaches, *Rev. Geophys.*, 52, 218–242, doi:10.1002/2013rg000443, 2014a.
- Hartmann, A., Kobler, J., Kralik, M., Dirnböck, T., Humer, F., and Weiler, M.: Transit time distributions to understand the biogeochemical impacts of storm Kyrill on an Austrian karst system, *Biogeosciences Discuss.*, in preparation, 2014b.
- Hartmann, A., Mudarra, M., Andreo, B., Marín, A., Wagener, T., and Lange, J.: Modeling spatiotemporal impacts of hydroclimatic extremes on groundwater recharge at a Mediterranean karst aquifer, *Water Resour. Res.*, 50, 6507–6521, doi:10.1002/2014WR015685, 2014c.
- Hatipoglu-Bagci, Z. and Sazan, M. S.: Characteristics of karst springs in Aydincik (Mersin, Turkey), based on recession curves and hydrochemical and isotopic parameters, *Q. J. Eng. Geol. Hydrogeol.*, 47, 89–99, 2014.
- Heilman, J. L., Litvak, M. E., McInnes, K. J., Kjelgaard, J. F., Kamps, R. H., and Schwinning, S.: Water-storage capacity controls energy partitioning and water use in karst ecosystems on the Edwards Plateau, Texas, *Ecohydrology*, 7, 127–138, doi:10.1002/eco.1327, 2014.
- Hirabayashi, Y., Mahendran, R., Koitala, S., Konoshima, L., Yamazaki, D., Watanabe, S., Kim, H., and Kanae, S.: Global flood risk under climate change, *Nat. Clim. Chang.*, 3, 816–821, doi:10.1038/nclimate1911, 2013.
- Jeannin, P.-Y. and Grasso, D. A.: Permeability and hydrodynamic behavior of karstic environment, in: *Karst Waters Environmental Impact*, edited by: Gunay, G. and Johnson, A. I., A. A. Balkema, Rotterdam, 335–342, 1997.

Simulation of groundwater recharge over Europe's karst regions

A. Hartmann et al.

[Title Page](#)

[Abstract](#)

[Introduction](#)

[Conclusions](#)

[References](#)

[Tables](#)

[Figures](#)

[◀](#)

[▶](#)

[◀](#)

[▶](#)

[Back](#)

[Close](#)

[Full Screen / Esc](#)

[Printer-friendly Version](#)

[Interactive Discussion](#)



- Jukic, D. and Denic-Jukic, V.: Estimating parameters of groundwater recharge model in frequency domain: karst springs Jadro and Žrnovnica, *Hydrol. Process.*, 22, 4532–4542, 2008.
- Ketchen, D. J. and Shook, C. L.: The application of cluster analysis, *Strateg. Manage. J.*, 17, 441–458, 1996.
- 5 Kiraly, L.: Modelling karst aquifers by the combined discrete channel and continuum approach, *Bull. d'Hydrogéologie*, 16, 77–98, 1998.
- Kiraly, L.: Karstification and Groundwater Flow, *Speleogenes. Evol. Karst Aquifers*, 1, 1–24, 2003.
- 10 Kirtman, B., Power, S. B., Adedoyin, J. A., Boer, G. J., Bojariu, R., Camilloni, I., Doblas-Reyes, F. J., Fiore, A. M., Kimoto, M., and Meehl, G. A.: Near-term climate change: projections and predictability, in: *Climate Change 2013: The Physical Science Basis, Contribution of Working Group I to the Fifth Assessment Report of the Intergovernmental Panel on Climate Change*, edited by: Stocker, T. F., Qin, D., Plattner, G.-K., Tignor, M., Allen, S. K., Boschung, J., Nauels, A., Xia, Y., Bex, V., and Midgley, P. M., Cambridge University Press, Cambridge, UK and New York, NY, USA, 953–1028, 2013.
- 15 Kottek, M., Grieser, J., Beck, C., Rudolf, B., and Rubel, F.: World Map of the Köppen-Geiger climate classification updated, *Meteorol. Z.*, 15, 259–263, doi:10.1127/0941-2948/2006/0130, 2006.
- Koutroulakis, A. G., Tsanis, I. K., Daliakopoulos, I. N., and Jacob, D.: Impact of climate change 20 on water resources status: a case study for Crete Island, Greece, *J. Hydrol.*, 479, 146–158, doi:10.1016/j.jhydrol.2012.11.055, 2013.
- Lange, J., Greenbaum, N., Husary, S., Ghanem, M., Leibundgut, C., and Schick, A. P.: Runoff generation from successive simulated rainfalls on a rocky, semi-arid, Mediterranean hillslope, *Hydrol. Process.*, 17, 279–296, doi:10.1002/hyp.1124, 2003.
- 25 Lee, E. S. and Krothe, N. C.: A four-component mixing model for water in a karst terrain in south-central Indiana, USA, using solute concentration and stable isotopes as tracers, *Chem. Geol.*, 179, 129–143, 2001.
- Leibowitz, S. G., Comeleo, R. L., Wigington Jr., P. J., Weaver, C. P., Morefield, P. E., Sproles, E. A., and Ebersole, J. L.: Hydrologic landscape classification evaluates streamflow 30 vulnerability to climate change in Oregon, USA, *Hydrol. Earth Syst. Sci.*, 18, 3367–3392, doi:10.5194/hess-18-3367-2014, 2014.
- Lerner, D. N., Issar, A. S., and Simmers, I.: *Groundwater Recharge: a Guide to Understanding and Estimating Natural Recharge*, Heise, Hannover, 1990.

Simulation of groundwater recharge over Europe's karst regions

A. Hartmann et al.

[Title Page](#)

[Abstract](#)

[Introduction](#)

[Conclusions](#)

[References](#)

[Tables](#)

[Figures](#)



[Back](#)

[Close](#)

[Full Screen / Esc](#)

[Printer-friendly Version](#)

[Interactive Discussion](#)

Simulation of groundwater recharge over Europe's karst regions

A. Hartmann et al.

[Title Page](#)

[Abstract](#)

[Introduction](#)

[Conclusions](#)

[References](#)

[Tables](#)

[Figures](#)

◀

▶

◀

▶

[Back](#)

[Close](#)

[Full Screen / Esc](#)

[Printer-friendly Version](#)

[Interactive Discussion](#)

Toll, D.: The Global Land Data Assimilation System, *B. Am. Meteorol. Soc.*, 85, 381–394, doi:10.1175/BAMS-85-3-381, 2004.

Rui, H. and Beaudoing, H.: README Document for Global Land Data Assimilation System Version 2 (GLDAS-2) Products, GES DISC/HSL, available at: <http://hydro1.sci.gsfc.nasa.gov/data/s4pa/GLDAS/README.GLDAS2.pdf> (last access: 17 November 2014), 2013.

5 Saltelli, A., Ratto, M., Andres, T., Campolongo, F., Cariboni, J., Gatelli, D., Saisana, M., and Tarantola, S.: *Global Sensitivity Analysis: The Primer*, John Wiley & Sons, 2008.

10 Samuels, R., Rimmer, A., Hartmann, A., Krichak, S., and Alpert, P.: Climate change impacts on Jordan River flow: downscaling application from a regional climate model, *J. Hydrometeorol.*, 11, 860–879, doi:10.1175/2010JHM1177.1, 2010.

Sawicz, K., Wagener, T., Sivapalan, M., Troch, P. A., and Carrillo, G.: Catchment classification: empirical analysis of hydrologic similarity based on catchment function in the eastern USA, *Hydrol. Earth Syst. Sci.*, 15, 2895–2911, doi:10.5194/hess-15-2895-2011, 2011.

15 Scanlon, B., Healy, R., and Cook, P.: Choosing appropriate techniques for quantifying ground-water recharge, *Hydrogeol. J.*, 10, 18–39, doi:10.1007/s10040-001-0176-2, 2002.

Seber, G. A. F.: *Multivariate Observations*, John Wiley & Sons, 2009.

20 Sivapalan, M., Yaeger, M. A., Harman, C. J., Xu, X., and Troch, P. A.: Functional model of water balance variability at the catchment scale: 1. Evidence of hydrologic similarity and space–time symmetry, *Water Resour. Res.*, 47, W02522, doi:10.1029/2010WR009568, 2011.

Spear, R. C. and Hornberger, G. M.: Eutrophication in peat inlet – II. Identification of critical uncertainties via generalized sensitivity analysis, *Water Resour. Res.*, 14, 43–49, 1980.

25 Tague, C. and Grant, G. E.: Groundwater dynamics mediate low-flow response to global warming in snow-dominated alpine regions, *Water Resour. Res.*, 45, W07421, doi:10.1029/2008WR007179, 2009.

Tritz, S., Guinot, V., and Jourde, H.: Modelling the behaviour of a karst system catchment using non-linear hysteretic conceptual model, *J. Hydrol.*, 397, 250–262, doi:10.1016/j.jhydrol.2010.12.001, 2011.

30 Vaute, L., Drogue, C., Garrelly, L., and Ghelfenstein, M.: Relations between the structure of storage and the transport of chemical compounds in karstic aquifers, *J. Hydrol.*, 199, 221–238, 1997.

- Viviroli, D., Dürr, H. H., Messerli, B., Meybeck, M., and Weingartner, R.: Mountains of the world, water towers for humanity: typology, mapping, and global significance, *Water Resour. Res.*, 43, W07447, doi:10.1029/2006WR005653, 2007.
- 5 Wada, Y., van Beek, L. P. H., van Kempen, C. M., Reckman, J. W. T. M., Vasak, S., and Bierkens, M. F. P.: Global depletion of groundwater resources, *Geophys. Res. Lett.*, 37, L20402, doi:10.1029/2010gl044571, 2010.
- Wada, Y., Wisser, D., and Bierkens, M. F. P.: Global modeling of withdrawal, allocation and consumptive use of surface water and groundwater resources, *Earth Syst. Dynam.*, 5, 15–40, doi:10.5194/esd-5-15-2014, 2014.
- 10 Wagener, T., Sivapalan, M., Troch, P. A., McGlynn, B. L., Harman, C. J., Gupta, H. V., Kumar, P., Rao, P. S. C., Basu, N. B., and Wilson, J. S.: The future of hydrology: an evolving science for a changing world, *Water Resour. Res.*, 46, W05301, doi:10.1029/2009wr008906, 2010.
- 15 Wigington, P. J., Leibowitz, S. G., Comeleo, R. L., and Ebersole, J. L.: Oregon hydrologic landscapes: a classification framework 1, *J. Am. Water Resour. Assoc.*, 49, 163–182, doi:10.1111/jawr.12009, 2013.
- Williams, P. W.: The role of the subcutaneous zone in karst hydrology, *J. Hydrol.*, 61, 45–67, 1983.
- Williams, P. W. and Ford, D. C.: Global distribution of carbonate rocks, *Z. Geomorphol.*, 147, 1–2, 2006.
- 20 Winter, T. C.: The concept of hydrologic landscapes, *JAWRA J. Am. Water Resour. Assoc.*, 37, 335–349, doi:10.1111/j.1752-1688.2001.tb00973.x, 2001.
- Wood, E. F., Roundy, J. K., Troy, T. J., van Beek, L. P. H., Bierkens, M. F. P., Blyth, E., de Roo, A., Döll, P., Ek, M., Famiglietti, J., Gochis, D., van de Giesen, N., Houser, P., Jaffé, P. R., Kollet, S., Lehner, B., Lettenmaier, D. P., Peters-Lidard, C., Sivapalan, M., Sheffield, J., Wade, A., and Whitehead, P.: Hyperresolution global land surface modeling: meeting a grand challenge for monitoring Earth's terrestrial water, *Water Resour. Res.*, 47, W05301, doi:10.1029/2010WR010090, 2011.

Simulation of groundwater recharge over Europe's karst regions

A. Hartmann et al.

[Title Page](#)

[Abstract](#)

[Introduction](#)

[Conclusions](#)

[References](#)

[Tables](#)

[Figures](#)



[Back](#)

[Close](#)

[Full Screen / Esc](#)

[Printer-friendly Version](#)

[Interactive Discussion](#)

Simulation of groundwater recharge over Europe's karst regions

A. Hartmann et al.

Table 1. Data availability, data properties and sources.

| Variable | Spatial resolution | Time period | Frequency | Source | Reference |
|-----------------------|----------------------|--------------------|-----------|------------------|------------------------------------------------|
| Precipitation | 0.25° | 2002–2012 | daily | GLDAS-2 | Rodell et al. (2004); Rui and Beaudoing (2013) |
| Temperature | 0.25° | 2002–2012 | daily | GLDAS-2 | |
| Net radiation | 0.25° | 2002–2012 | daily | GLDAS-2 | |
| Snow water equivalent | 0.25° | 2002–2012 | daily | NOAHv3.3/GLDAS-2 | Ek (2003); Rodell et al. (2004) |
| Carbonate rock areas | vector data | – | – | | Williams and Ford (2006) |
| Elevation | 3" | – | – | SRMT V2.1 | Farr et al. (2007) |
| Rock permeability | vector data | – | – | | Gleeson et al. (2014) |
| Actual evaporation | individual locations | individual periods | daily | FLUXNET | Baldocchi et al. (2001) |
| Soil moisture | Individual locations | individual periods | daily | ISMN | Dorigo et al. (2011) |

- [Title Page](#)
- [Abstract](#) [Introduction](#)
- [Conclusions](#) [References](#)
- [Tables](#) [Figures](#)
- [◀](#) [▶](#)
- [◀](#) [▶](#)
- [Back](#) [Close](#)
- [Full Screen / Esc](#)
- [Printer-friendly Version](#)
- [Interactive Discussion](#)

Simulation of groundwater recharge over Europe's karst regions

A. Hartmann et al.

Table 2. Initial parameter ranges for Monte Carlo sampling based on previous field studies and large-scale model applications.

| Parameter | Unit | Lower limit | Upper limit | References |
|-------------------|------|-------------|-------------|----------------------------------------------------------------------|
| a | [–] | 0 | 6 | Hartmann et al. (2013b, 2014b, d) |
| V_{soil} | [mm] | 0 | 1250 | Miralles et al. (2011); FAO/IIASA/ISRIC/ISSCAS/JRCv, 2012; Ek (2003) |
| V_{epi} | [mm] | 200 | 700 | Perrin et al. (2003), Williams (2008) |
| K_{epi} | [d] | 0 | 50 | Gleeson et al. (2014), Hartmann et al. (2013b) |



Simulation of groundwater recharge over Europe's karst regions

A. Hartmann et al.

[Title Page](#)

[Abstract](#)

[Introduction](#)

[Conclusions](#)

[References](#)

[Tables](#)

[Figures](#)

◀

▶

◀

▶

[Back](#)

[Close](#)

[Full Screen / Esc](#)

[Printer-friendly Version](#)

[Interactive Discussion](#)

Table 3. Independent observations of mean annual recharge from field and modelling studies over Europe.

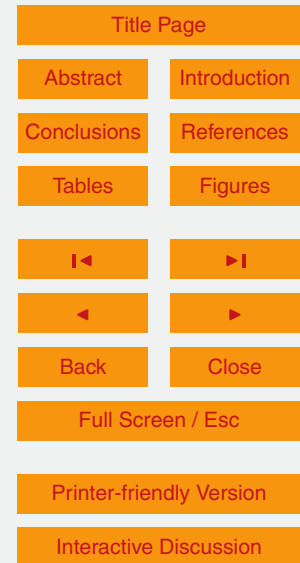
| Location (country, province) | Latitude [dec. degr.] | Longitude [dec. degr.] | Mean annual recharge [mm] | Method | Author |
|----------------------------------------------------|--------------------------|---------------------------|------------------------------|---------------------------|----------------------------------|
| UK (Greta spring, Durham) | 54.52 | -1.87 | 690 | observed water balance | Arnell (2003) |
| UK (Lambourn) | 51.5 | -1.53 | 234 | observed water balance | Arnell (2003) |
| UK (R. Teme, Tenbury wells) | 52.3 | -2.58 | 355 | observed water balance | Arnell (2003) |
| Spain (Cazorla, Sierra de Cazorla) | 37.9 | -3.03 | 244 | empiric estimation method | Andre et al. (2008) |
| Spain (Sierra de las Cabras, Arcos de la frontera) | 36.65 | -5.72 | 318 | empiric estimation method | Andre et al. (2008) |
| Fr (Fontaine de Vaucluse) | 43.92 | 5.13 | 568 | observed water balance | Fleury et al. (2007) |
| Fr (Bonneire, La Rouchefoucauld-Touvre) | 45.8 | 0.44 | 250 | simulated water balance | Le Moine et al. (2007) |
| Fr (Durzon spring, La Cavalerie) | 44.01 | 3.16 | 378 | observed water balance | Tritz et al. (2011) |
| Ger (Gallusquelle spring, Swabian Albs) | 48.21 | 9.15 | 351 | observed water balance | Doummar et al. (2012) |
| Ger (Bohming spring, Rieshofen) | 48.93 | 11.3 | 130 | observed water balance | Einsiedl (2005) |
| Greece (Arvi, Crete)* | 35.13 | 24.55 | 241 | observed water balance | Koutoulis et al. (2013) |
| Italy (Cerella spring, Latina) | 41.88 | 12.9 | 416 | empiric estimation method | Allocata et al. (2014) |
| Italy (Forcella spring, Sapri) | 41.05 | 14.55 | 559 | empiric estimation method | Allocata et al. (2014) |
| Italy (Taburno spring) | 39.9 | 15.81 | 693 | empiric estimation method | Allocata et al. (2014) |
| Croatia (Jadro spring, Dugopolje) | 43.58 | 16.6 | 795 | simulated water balance | Jukic and Denic-Jukic (2008) |
| Turkey (Harmankoy, Beyyayla) | 40.15 | 30.65 | 32 | observed water balance | (Aydin et al., 2013) |
| Turkey (Aydincik, Mersin) | 36.97 | 33.22 | 552 | observed water balance | Hatipoglu-Bagci and Sazan (2014) |
| Italy (Gran Sasso, Teramo) | 42.27 | 13.34 | 700 | observed water balance | Barbieri et al. (2005) |
| Austria (Siebenquellen spring, Schneeaple) | 47.69 | 15.6 | 694 | observed water balance | Maloszewski et al. (2002) |
| Spain (La Villa spring, El Torcel) | 36.93 | -4.52 | 463 | observed water balance | Padilla et al. (1994) |
| Croatia (St. Ivan, Mirna) | 45.22 | 13.6 | 386 | observed water balance | Bonacci (2001) |
| France (St Hippolyte-du-Fort, Vidourle) | 43.93 | 3.85 | 287 | observed water balance | Vaute et al. (1997) |

Simulation of groundwater recharge over Europe's karst regions

A. Hartmann et al.

Table 4. Cluster means of the 4 identified karst landscapes.

| descriptor | unit | number of cluster/karst landscape | | | |
|------------|--------------------|-----------------------------------|-------|-------|-------|
| | | 1.HUM | 2.MTN | 3.MED | 4.DES |
| AI | [–] | 0.80 | 0.98 | 3.18 | 20.00 |
| DS | [a ⁻¹] | 85 | 76 | 16 | 1 |
| RA | [m] | 228 | 1785 | 691 | 232 |



Simulation of groundwater recharge over Europe's karst regions

A. Hartmann et al.

Table 5. Minima and maxima of the confined parameter samples for each of the identified landscapes.

| Parameter | Unit | HUM | | MTN | | MED | | DES | |
|------------------------------|------|----------------|------------------|----------------|----------------|--------------|----------------|------------|---------------|
| | | min | max | min | max | min | max | min | max |
| a | [–] | 1.1 | 3.3 | 0.3 | 2.9 | 0.8 | 6.0 | 0.1 | 6.0 |
| $V_{\text{soil}}^{\text{a}}$ | [mm] | 900.1 (900) | 1248.9 (1250) | 500.4 (500) | 899.9 (900) | 51.7 (50) | 498.4 (500) | 0.2 (0) | 49.1 (500) |
| V_{epi} | [mm] | 204.3 | 694.8 | 201.6 | 699.4 | 200.1 | 696.7 | 202.3 | 695.7 |
| K_{epi} | [d] | 0.0 | 35.8 | 7.3 | 49.9 | 0.0 | 48.4 | 10.4 | 49.9 |

^a In brackets: a priori information used for step 3 of the parameter confinement strategy.

Title Page

Abstract

Introduction

Conclusions

References

Tables

Figures

◀

▶

◀

▶

Back

Close

Full Screen / Esc

Printer-friendly Version

Interactive Discussion

Simulation of groundwater recharge over Europe's karst regions

A. Hartmann et al.

Table 6. Mean deviations of the VarKarst-R, the PCR-GLOBWB model and the WaterGAP model from all observations and the individual regions.

| region | mean deviation [mm a^{-1}] | | |
|------------------|---------------------------------------|------------|----------|
| | VarKarst-R | PCR-GLOBWB | WaterGAP |
| all | -22.0 | 203.9 | -273.3 |
| HUM ($n = 10$) | 121.5 | -131.4 | -149.2 |
| MTN ($n = 7$) | -192.2 | -333.6 | -446.4 |
| MED ($n = 7$) | -52.6 | -252.9 | -277.6 |

-
- [Title Page](#)
-
- [Abstract](#) [Introduction](#)
-
- [Conclusions](#) [References](#)
-
- [Tables](#) [Figures](#)
-
- ◀ ▶
-
- ◀ ▶
-
- [Back](#) [Close](#)
-
- [Full Screen / Esc](#)
-
- [Printer-friendly Version](#)
-
- [Interactive Discussion](#)

Simulation of groundwater recharge over Europe's karst regions

A. Hartmann et al.

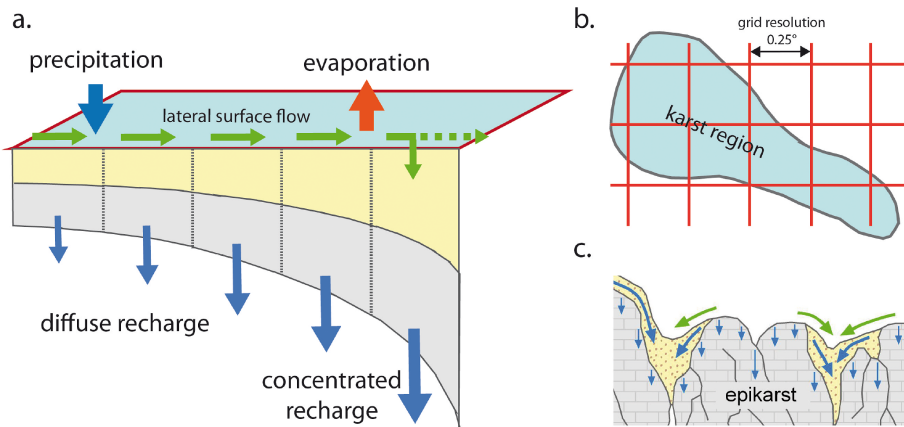


Figure 1. (a) schematic description of the model, (b) its gridded discretisation over karst regions and (c) the subsurface heterogeneity that its structure represents for each grid cell.

Simulation of groundwater recharge over Europe's karst regions

A. Hartmann et al.

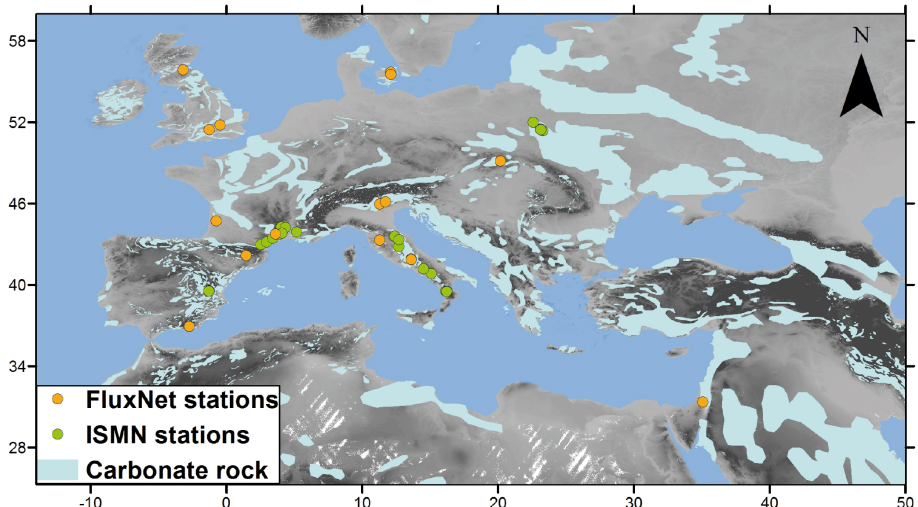


Figure 2. Carbonate rock areas over Europe and location of the selected FLUXNET and ISMN stations.

- [Title Page](#)
- [Abstract](#) [Introduction](#)
- [Conclusions](#) [References](#)
- [Tables](#) [Figures](#)
- [◀](#) [▶](#)
- [◀](#) [▶](#)
- [Back](#) [Close](#)
- [Full Screen / Esc](#)
- [Printer-friendly Version](#)
- [Interactive Discussion](#)

Simulation of groundwater recharge over Europe's karst regions

A. Hartmann et al.

| | |
|------------------------------------------|------------------------------|
| Title Page | |
| Abstract | Introduction |
| Conclusions | References |
| Tables | Figures |
| ◀ | ▶ |
| ◀ | ▶ |
| Back | Close |
| Full Screen / Esc | |
| Printer-friendly Version | |
| Interactive Discussion | |

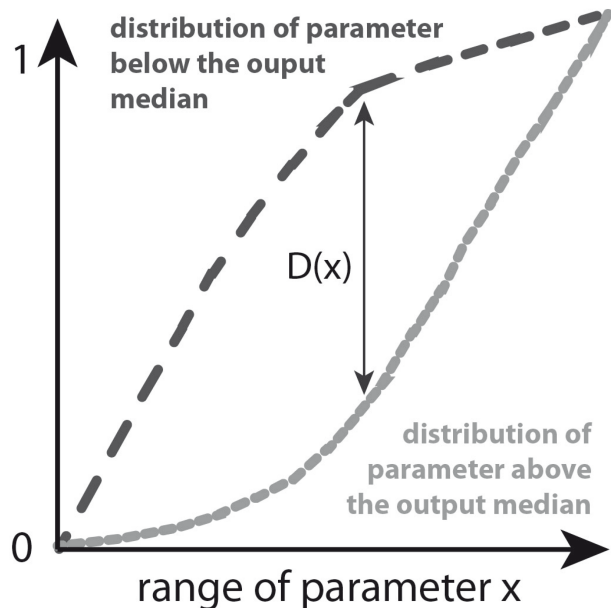


Figure 3. Schematic elaboration of the regional sensitivity analysis procedure.

Simulation of groundwater recharge over Europe's karst regions

A. Hartmann et al.

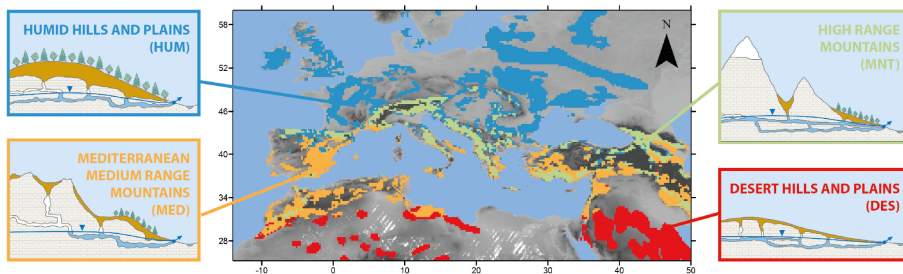


Figure 4. Map with clusters over Europe and typical karst landscapes that were attributed to them.

- [Title Page](#)
- [Abstract](#) [Introduction](#)
- [Conclusions](#) [References](#)
- [Tables](#) [Figures](#)
- [◀](#) [▶](#)
- [◀](#) [▶](#)
- [Back](#) [Close](#)
- [Full Screen / Esc](#)
- [Printer-friendly Version](#)
- [Interactive Discussion](#)

Simulation of groundwater recharge over Europe's karst regions

A. Hartmann et al.

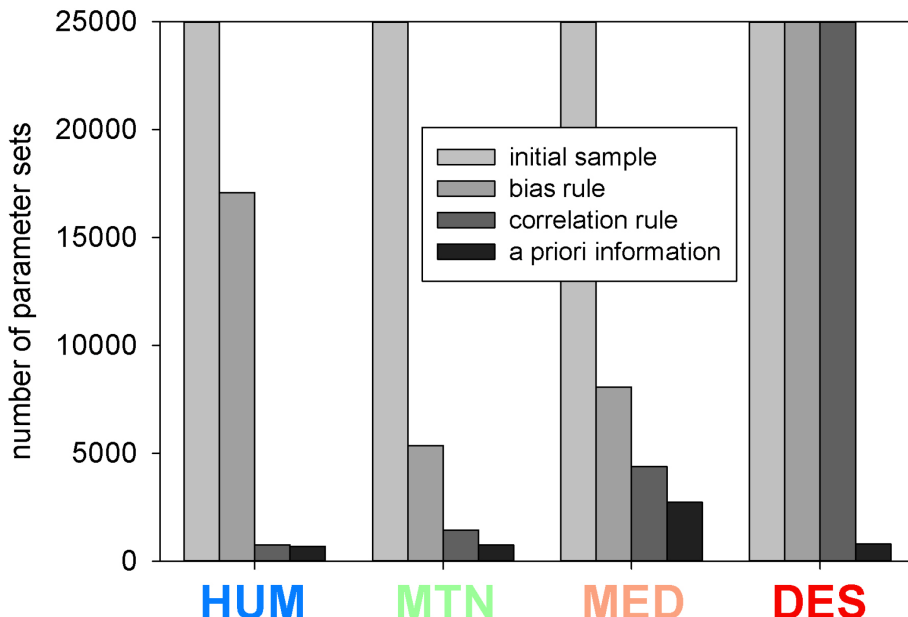


Figure 5. Evolution of the initial sample of 25 000 parameter sets along the different confinement steps for the 4 karst landscapes.

- [Title Page](#)
- [Abstract](#) [Introduction](#)
- [Conclusions](#) [References](#)
- [Tables](#) [Figures](#)
- [◀](#) [▶](#)
- [◀](#) [▶](#)
- [Back](#) [Close](#)
- [Full Screen / Esc](#)
- [Printer-friendly Version](#)
- [Interactive Discussion](#)

Simulation of groundwater recharge over Europe's karst regions

A. Hartmann et al.

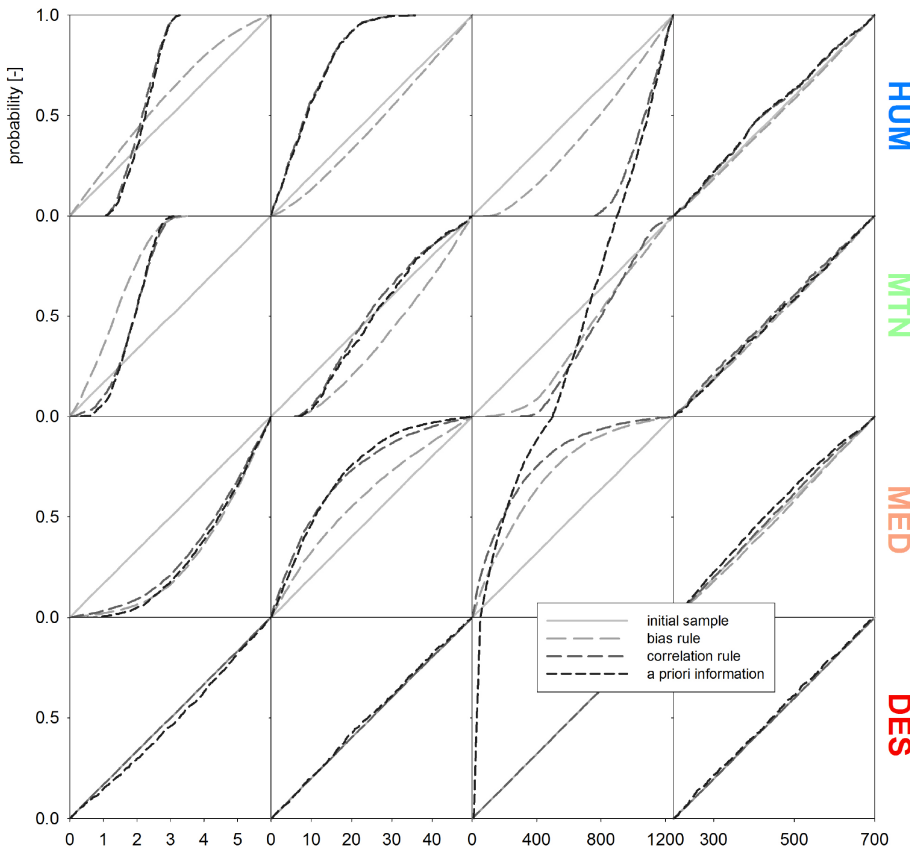


Figure 6. Evolution of posterior probabilities of the 4 model parameters for the 4 karst landscapes along the steps of the parameter confinement strategy.

Simulation of groundwater recharge over Europe's karst regions

A. Hartmann et al.

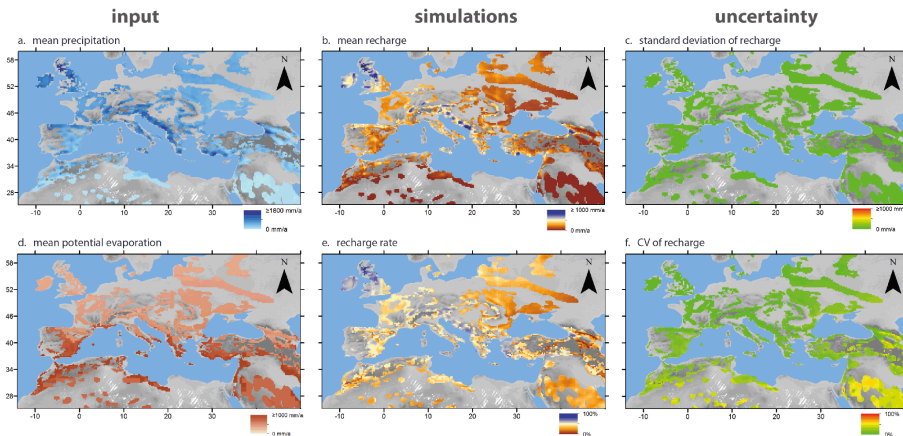


Figure 7. (a) Observed precipitation and (d) potential evaporation vs. the simulated (b) mean annual recharge and (e) mean annual recharge rates derived from the mean of all 250 parameter sets, and (c) the SD and (f) coefficients of variation of the simulations due to the variability among the 250 parameter sets.

Simulation of groundwater recharge over Europe's karst regions

A. Hartmann et al.

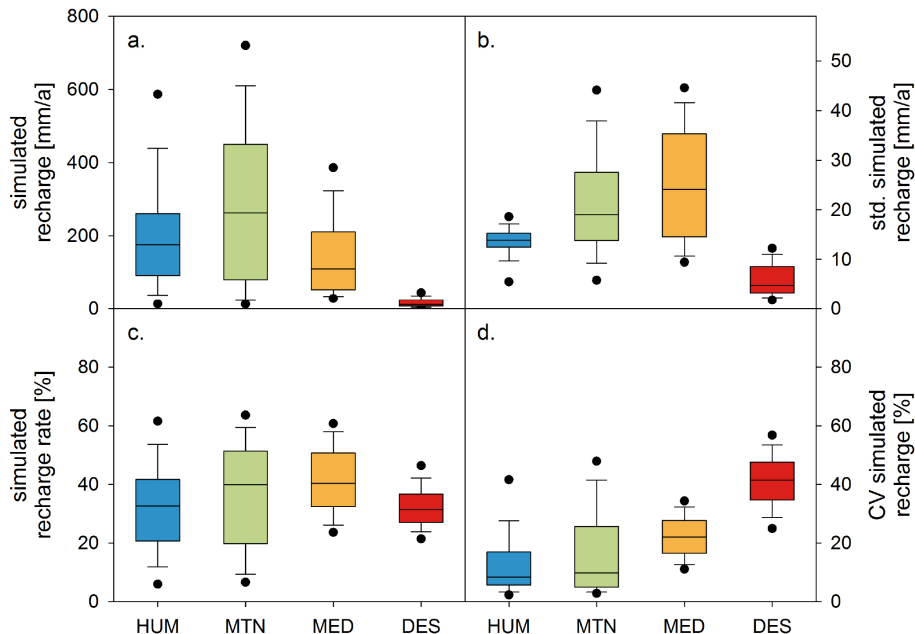


Figure 8. (a) Simulated mean annual recharge, among the 4 karst landscapes, (b) their SDs, (c) recharge rates, and (d) coefficients of variation obtained by the final sample of parameters.

- [Title Page](#)
- [Abstract](#) [Introduction](#)
- [Conclusions](#) [References](#)
- [Tables](#) [Figures](#)
- [◀](#) [▶](#)
- [◀](#) [▶](#)
- [Back](#) [Close](#)
- [Full Screen / Esc](#)
- [Printer-friendly Version](#)
- [Interactive Discussion](#)

Simulation of groundwater recharge over Europe's karst regions

A. Hartmann et al.

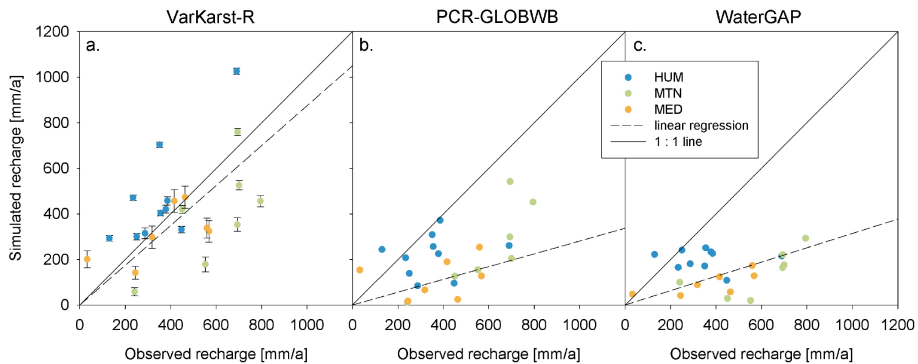


Figure 9. Observations of mean annual recharge from independent studies vs. the simulated mean annual recharge by the VarKarst-R and the PCR-GLOBWB model (no data for the DES region available).

- [Title Page](#)
- [Abstract](#) [Introduction](#)
- [Conclusions](#) [References](#)
- [Tables](#) [Figures](#)
- [◀](#) [▶](#)
- [◀](#) [▶](#)
- [Back](#) [Close](#)
- [Full Screen / Esc](#)
- [Printer-friendly Version](#)
- [Interactive Discussion](#)

Simulation of groundwater recharge over Europe's karst regions

A. Hartmann et al.

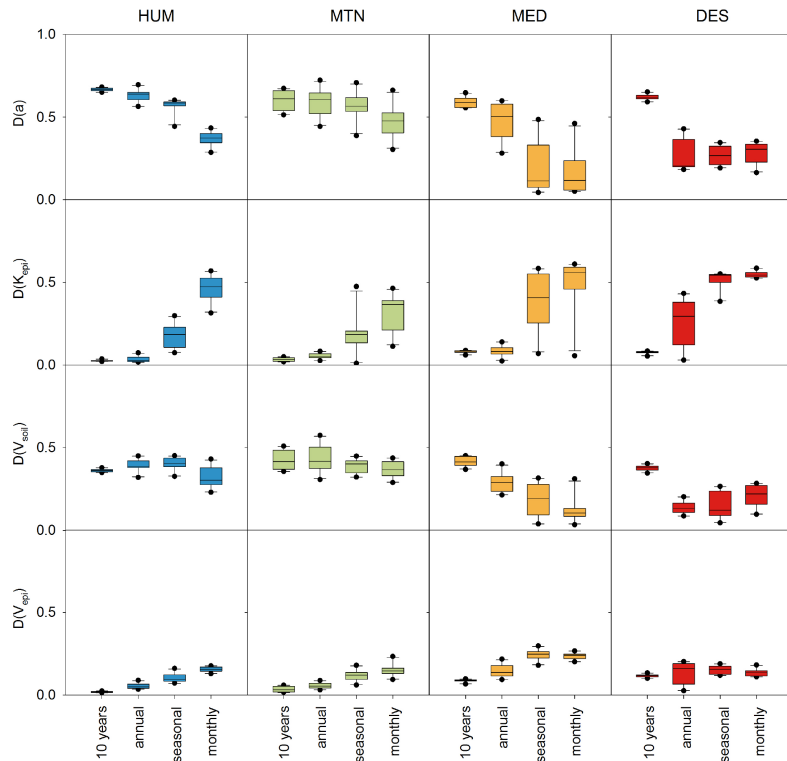


Figure 10. Sensitivity of simulated recharge to the model parameters at different time scales and in the different karst landscapes. Sensitivity is measured by the maximum distance (D) between the distribution of parameter sets that produce “low” recharge (i.e. below the median) and the distribution producing “high” recharge (above the median). Parameter sets are initially sampled from the ranges in Table 2.

- [Title Page](#)
- [Abstract](#) [Introduction](#)
- [Conclusions](#) [References](#)
- [Tables](#) [Figures](#)
- [◀](#) [▶](#)
- [◀](#) [▶](#)
- [Back](#) [Close](#)
- [Full Screen / Esc](#)
- [Printer-friendly Version](#)
- [Interactive Discussion](#)

Simulation of groundwater recharge over Europe's karst regions

A. Hartmann et al.

- [Title Page](#)
- [Abstract](#) [Introduction](#)
- [Conclusions](#) [References](#)
- [Tables](#) [Figures](#)
- [◀](#) [▶](#)
- [◀](#) [▶](#)
- [Back](#) [Close](#)
- [Full Screen / Esc](#)
- [Printer-friendly Version](#)
- [Interactive Discussion](#)

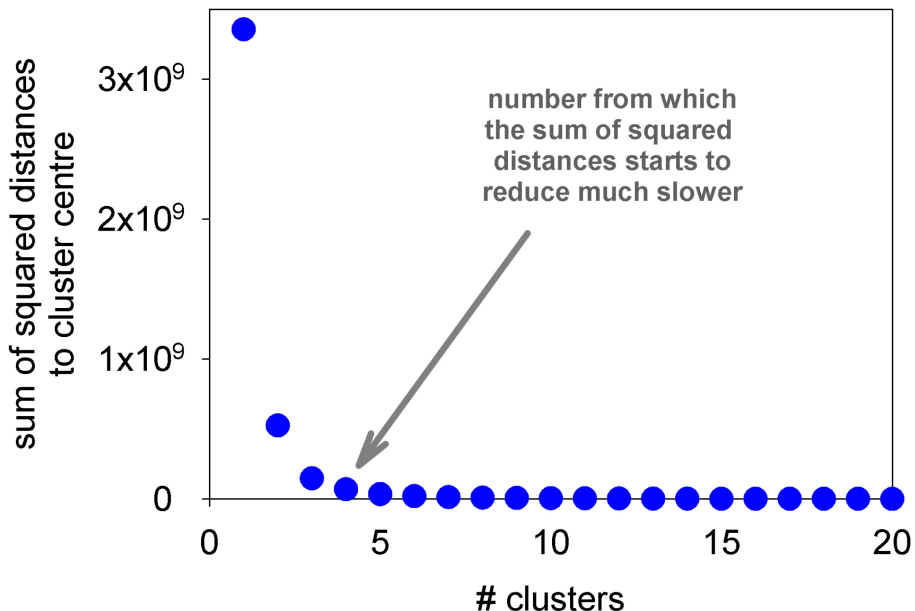


Figure A1. Elbow plot of sum of squared distances to cluster centres for k means method.

Simulation of groundwater recharge over Europe's karst regions

A. Hartmann et al.

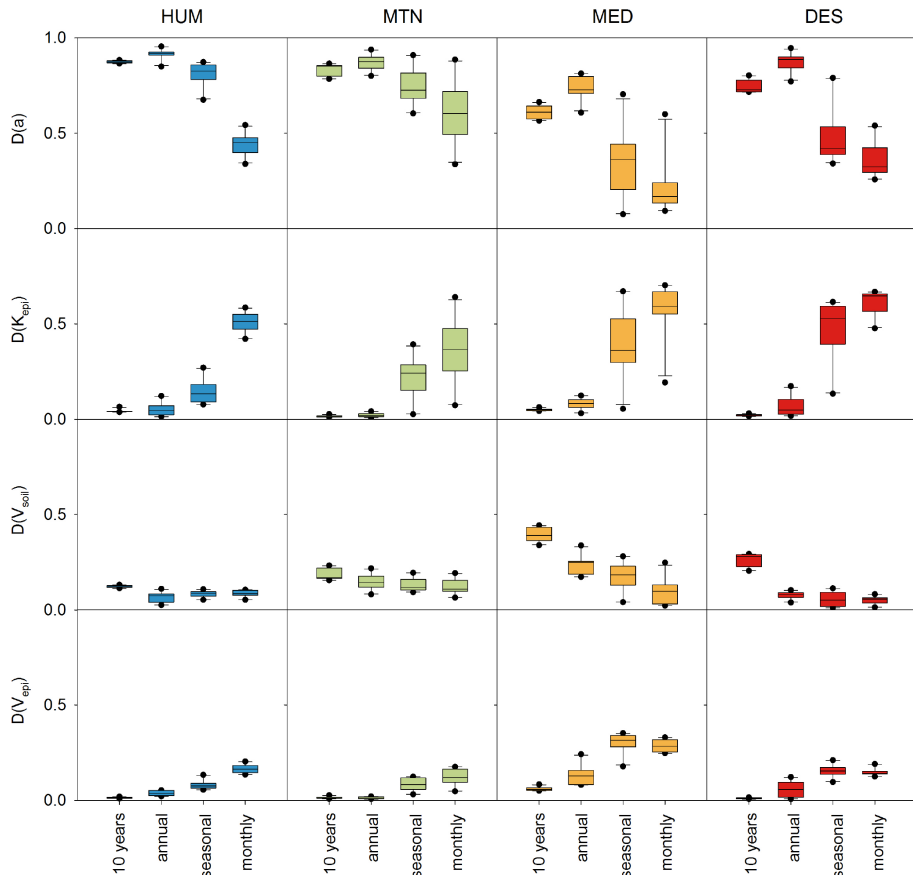


Figure A2. Sensitivity of simulated recharge to the model parameters at different time scales and in the different karst landscapes, as in Fig. 10 but sampling parameters from the confined parameter ranges of Table 5.